Modelling study on phase equilibria behavior of ionic liquid-based aqueous biphasic systems

Chen, Yuqiu; Liang, Xiaodong; Woodley, John M.; Kontogeorgis, Georgios M.

Published in:
Chemical Engineering Science

Link to article, DOI:
10.1016/j.ces.2021.116904

Publication date:
2022

Document Version
Publisher's PDF, also known as Version of record

Chemical Engineering Science 247 (2022) 116904

Contents lists available at ScienceDirect

Chemical Engineering Science

journal homepage: www.elsevier.com/locate/ces

Modelling study on phase equilibria behavior of ionic liquid-based aqueous biphasic systems

Yuqiu Chen, Xiaodong Liang, John M. Woodley, Georgios M. Kontogeorgis *

Department of Chemical and Biochemical Engineering, Technical University of Denmark, DK-2800 Lyngby, Denmark

HIGHLIGHTS

- 17,449 experimental binodal data points covering various IL-ABS at different temperatures are collected.
- Optimal parameters of a well-known mathematical description for each of the IL-ABS are obtained.
- A machine learning model (ANN-GC) with reliable predictive performance is developed.
- Some main issues that govern the phase equilibria behavior of IL- ABS are discussed.

ARTICLE INFO

Article history:
Received 2 April 2021
Received in revised form 18 June 2021
Accepted 28 June 2021
Available online 1 July 2021

Keywords:
Ionic liquids
ABS
Group contribution
Matching learning
Artificial neural network

ABSTRACT

The ability to predict the phase equilibria behavior is of crucial relevance in the early design stage of biphasic liquid-liquid systems. Ionic liquid-based aqueous biphasic systems (IL-ABS) have demonstrated superior performance in many applications such as the recovery of bio-products and the recycling of hydrophilic ILs from aqueous solutions. In order to better utilize these novel biphasic liquid-liquid systems, modelling studies on phase equilibria behavior are carried out in this work. First, the IL database developed in our previous work is extended to these unconventional biphasic systems. In total, 17,449 experimental binodal data points covering 171 IL-ABS at different temperatures (278.15 K-343.15 K) are collected. Then, all involved IL-ABS are correlated using a popular three-parameter mathematical description and the optimal parameters of each IL-ABS are obtained. Afterwards, we try to build a linear group contribution (GC) model to predict the phase equilibria behavior of IL-ABS, but it fails due to the high complexity of these biphasic systems. For this reason, we finally turn to applying a well-known machine learning algorithm, i.e., artificial neural network (ANN), to build a nonlinear GC model for such a purpose. This model gives a mean absolute error (MAE) of 0.0175 and squared correlation coefficient (R^2) of 0.9316 for the 13,789 training data points, and for the 3,660 test data points they are 0.0177 and 0.9195, respectively. The results indicate that the proposed nonlinear ANN-GC model, to some extent, is capable to predict the phase equilibria behavior of IL-ABS. Besides the efforts of building GC models, we also discuss some main issues that govern the phase equilibria behavior of IL- ABS, which could be a guidance in the design of IL-ABS.

1. Introduction

Ionic liquids (ILs) are being considered as potential alternatives to conventional organic solvents due to their attractive properties such as negligible volatility, non-flammability, exhibiting good solubility and selectivity for a wide range of organic and inorganic chemicals (Rogers and Seddon, 2003). The replacement of volatile organic solvents by ILs is able to lower the energy consumption in solvent recycle and reduce the solvent loss to the atmosphere, thereby decreasing the environmental footprint and even reducing the cost of the process in some cases (Chen et al., 2019a, 2019b; Liu et al., 2020; Lei et al., 2021). Moreover, ILs have been recognized as "designer solvents" (Plechkova and Seddon, 2007) since their properties can be tailored by tuning the molecular structure and this feature allows the possibility of designing suitable ILs with desired properties for specific tasks. So far, ILs have been widely studied in many fields such as chemistry, pharmaceuticals and materials, where they can play different roles such as solvents in separations (Ventura, 2017), media and/or catalysts in reactions (Vekariya, 2017; Meng et al., 2019) and functional material (Liu and Jin, 2016).

* Corresponding author.
E-mail address: gk@kt.dtu.dk (G.M. Kontogeorgis).

https://doi.org/10.1016/j.ces.2021.116904
0009-2509/

Currently, IL-based separations are the most widely studied approaches involving ILs. Among them, IL-based liquid-liquid extractions (LLE) and IL-based aqueous biphasic systems (ABS) extractions are being paid more attention in many separation and purification processes, particularly in bioprocesses. To date, these separation approaches have been applied to recover various bioproducts ranging from small organic compounds (e.g., phenolic acids, alkaloids, amino acids, lipids and other hydrophobic compounds) (Bi et al., 2012; Freire et al., 2010, 2012; Pei et al., 2012; Zafarani-Moattar and Hamzehzadeh, 2011; Wu et al., 2015; Wang et al., 2005; Absalan et al., 2010; Yang et al., 2009, 2012, 2013; Liang et al., 2013) to more complex molecules (e.g., nucleic acids, proteins, enzymes, antibodies) (Fister et al., 2015; Pei et al., 2009; Lin et al., 2013; Quental et al., 2015; Yan et al., 2014; Ren et al., 2015; Xu et al., 2014; Ito et al., 2013; Dreyer and Kragl, 2008). A variety of ILs have been synthesized for such purposes by many researchers, especially Coutinho's group from University of Aveiro. Recently, a critical review on IL-mediated extraction and separation processes for bioactive compounds was published and it demonstrates that, if properly selected/designed, ILs can provide higher extraction yields and purification factors compared to conventional organic solvents (Ventura, 2017). Generally, LLE with hydrophobic water-immiscible ILs are initially used for water-rich biomass extracts (Absalan et al., 2008). However, the number of available hydrophobic ILs is much more limited when compared to hydrophilic ones and they tend to be very costly (Ventura, 2017). On the other hand, ABS with hydrophilic water-miscible ILs are usually recognized as biocompatible, non-denaturing and benign media for cells, cell organelles and biologically active substances, and they have demonstrated superior performance as alternative extraction platforms. So far, most of the successfully extractions using ILs for natural compounds recovery from biomass are carried out by this type of IL-based technique (Freire et al., 2012).

ABS refer to two aqueous-rich phases which are ternary systems composed of water and two solutes. They are clean alternatives for traditional organic-water solvent extraction systems and have gained an increasing interest due to their potential in biotechnological applications (Raja et al., 2011). The main advantages of ABS technique can be summarized as: (i) they provide mild conditions that do not harm or denature unstable/labile biomolecules; (ii) they enable rapid phase separation and compounds partition, and have far lower interfacial stress than water-organic solvent systems which allow less damage to the molecules to be extracted; (iii) specialized systems can be tailored by varying factors (e.g., temperature, presence of certain ions) to favor the enrichment of a specific compound into one of the two phases; (iv) they are able to give high recovery yield and is easily to scale up (Raja et al., 2011; Iqbal et al., 2016; Grilo et al., 2016; Goja et al., 2013). To date, ABS have been successfully used as non-denaturing and benign separation media to recover various biomolecules such as proteins, enzymes and antibiotics from crude cell extracts or other mixtures (Asenjo and Andrews, 2012; Nadar et al., 2017; Magalhães et al., 2020). However, challenges such as how to obtain reliable phase behavior predictions of ABS, how to reuse of the phase-forming components and how to incorporate other operation units in downstream processing need to be addressed to take their place at the industrial level (Magalhães et al., 2020). Besides these, find low cost, low toxicity and high-performance phase forming agents is another issue needs to be taken into account.

ABS with water-miscible ILs were firstly proposed by Rogers and co-workers (Gutowski et al., 2003) in 2003 and these systems are reported to have potential to replace the typical polymer-based ABS due to their unique system properties such as low toxicity, low viscosity, and tailored selectivity. The main applications of IL-based ABS can be summarized as: (i) the recovery and recycling of ILs from aqueous solutions, (ii) new separation techniques and (iii) carrying out metathesis reactions in the formation of new ILs (Freire, 2016). To date, most ILs investigated in ABS are composed of well-known cations (e.g., imidazolium, pyridinium, ammonium, phosphonium) and anions including halogens, sulphates, sulphonates, alkanoates, tetrafluoroborate and triflate. On the other hand, inorganic salts such as NaH_2PO_4, K_3PO_4 and $(NH_4)_2SO_4$ are the most widely used second phase-forming agents in IL-based ABS, while a certain number of more benign species such as organic salts, amino acids, carbohydrates and polymers are being studied as alternatives to high-charge-density inorganic salts in the formation of second phase (Ventura, 2017). As both IL and phase-forming agent have influence on the system's properties, it is challenging to rationally design IL-based ABS for specific tasks. Therefore, a systematic understanding of the relationship between the property of IL-based ABS and its composition is essential to promote its wide application. The optimal design of compounds through manipulating properties at the molecular level is often the key to considerable scientific advances and improved process systems performance (Alshehri et al., 2020). Recently, the computer-aided ionic liquid design (CAILD) method has been widely applied to design suitable ILs for various processing tasks (Song et al., 2018, 2019; Chen et al., 2018a, 2018b, 2020c; Liu et al., 2021). When using CAILD for the optimal design of IL-based ABS, the development of reliable models to describe the property of these systems is essential.

Rogers and co-workers (Gutowski et al., 2003) were the first to use a mathematical description (Eq. (1)) to correlate the experimental coexisting curve of IL-based ABS which was initially proposed by Merchuk et al. (Merchuk et al., 1998) to describe polymer-based ABS. Then, many researchers used Eq. (1) to describe various IL-based ABS since it can satisfactorily reproduce their experimental binodal boundaries. Zafarani-Moattar and Hamzehzadeh (Zafarani-Moattar and Hamzehzadeh, 2009, 2010) further expressed the dependence of the coefficients A, B and C of Eq. (1) as a function of temperature and as a function of pH, respectively. They found that these temperature/pH associated descriptions are able to provide good correlations of the binodal experimental curves with different temperature and pH. Nonetheless, current correlation studies of the binodal experimental curves are limited to a single ABS. It means that different IL-based ABS have their own correlation coefficients, and they cannot be used interchangeably. Therefore, a mathematical description with same coefficients that is capable to describe all IL-based ABS is highly desirable due to the fact it can provide quantitative information of structure–property for the optimal design of IL-based ABS. In this regard, group contribution (GC) methods may have the potential since both IL and phase-forming agent in ABS can be described as the occurrences of functional groups in the molecule. In addition, GC models can be easily combined in the computer-aided design method, (Gani, 2019) which make it possible to use CAILD for the optimal design of IL-based ABS.

Most properties are initially associated with the group numbers using a linear GC model. However, some of them cannot be properly described by linear model expressions and nonlinear GC models are needed to achieve more reliable predictions in such cases. In this respect, machine learning (ML) algorithms such as artificial neural networks (ANN) and support vector machine that are capable to build complex nonlinear GC or QSPR models have been widely used for various properties including gas solubility (Sedghamiz et al., 2015; Tatar et al., 2016; Faúndez et al., 2016; Zhao et al., 2016; Song et al., 2020), surface tension (Mulero et al., 2017) and toxicity of ILs (Cao et al., 2018; Wang et al., 2021). ANNs have also been used by many scientists in the phase equilibrium calculations. So far, no investigations of using GC methods to study IL-based ABS have been reported, it is the pur-

pose of this work to investigate such possibilities. Besides the efforts of building GC models, we also discuss some main issues that govern the phase equilibria behavior of IL- ABS, which could be a guidance in the design of IL-ABS.

2. Experimental data sets

For the purpose of building GC models to predict the phase equilibria behavior of IL-based ABS, the IL database developed in our previous works (Chen et al., 2019a, 2020b, 2020c) is extended to these unconventional aqueous biphasic systems. In total, 17,449 experimental binodal data points of 171 IL-based aqueous biphasic systems covering 56 ILs and 43 s phase-forming agents (summarized in Table 1) from 278.15 K to 343.15 K are collected. All involved IL-ABS together with their experimental binodal data are provided in the Supporting Information. Similar to our previous work of developing GC models for physical properties, (Chen et al., 2019a, 2020b, 2020c) IL molecules in ABS are also decomposed into three types of building groups (i.e., cation cores, cation substituents, anions) considering the design space and the flexibility of ILs. For the second phase-forming agents, organic/inorganic salts are decomposed into cations and anions, while amino acids and carbohydrates are regarded as whole molecular groups. It should be noted that cations and anions decomposed from ILs and organic/inorganic salts are different. In order to distinguish them, we use salt cation(s) and salt anion(s) to, represent the cations and anions decomposed from organic/inorganic salts in this work. Fig. 1 gives the structure of IL-ABS described by building blocks from the concept of GC model.

In total, 71 different building groups are obtained from the decomposition of all involved ILs and the second phase-forming agents, wherein 34 are IL building groups (6 cation cores, 23 anions, 5 substituents) and the remaining 37 groups belonging to the second phase-forming agents including inorganic/organic salts, carbohydrates, amino acids, as shown in Table 2. All building groups with their numbers of occurrence in each IL-ABS are given in the Supporting Information. Testing is an essential part of the model development and therefore we divide the experimental binodal data into a training set and a test set. The training set accounts for nearly 80% of the data points and the remaining data points (test set) are used to evaluate the predictive performance of the developed linear/nonlinear GC model. The training set and test set are, respectively, provided in Table S4 and Table S5 (Supporting Information).

3. Linear model

In this section, we use a three-parameter mathematical description, as shown in Eq. (1), to fit the experimental coexisting curves of IL-ABS. This equation was initially proposed by Merchuk et al. (Merchuk et al., 1998) to describe polymer-based aqueous biphasic systems and then Rogers and co-workers (Gutowski et al., 2003) were the first to introduce it to IL-based aqueous biphasic systems. Since then, this equation has been successfully applied to describe various IL-ABS. Zafarani-Moattar and Hamzehzadeh (Zafarani-Moattar and Hamzehzadeh, 2009, 2010) and Wang et al. (Wang et al., 2010) further extended this equation to IL-ABS with different temperatures and the three fitting parameters of Eq. (1) are expressed as a function of temperature in a linear form as Eqs. (2)–(4).

$$Y = A\exp\left[\left(B \times X^{0.5}\right) - \left(C \times X^{3}\right)\right] \tag{1}$$

where Y and X are the weight fraction percentages of the IL and the second phase-forming agent and A, B and C are fitting parameters which can be calculated from following T-dependent equations.

$$A = A^0 + A^1(T - T_0) \tag{2}$$

$$B = B^0 + B^1(T - T_0) \tag{3}$$

$$C = C^0 + C^1(T - T_0) \tag{4}$$

where T represents the temperature (K) of the studied ABS system and T_0 denotes the reference temperature (=273.15 K). A^0, A^1, B^0, B^1, C^0 and C^1 are T-independent adjustable parameters which can be directly obtained by correlating the experimental data points into Eq. (1) or can be indirectly calculated from Eq. (5) when using the GC-based linear model to describe the IL-ABS.

$$A^0 = \sum_{i=1}^{k} n_i a_i^0 B^0 = \sum_{i=1}^{k} n_i b_i^0 C^0 = \sum_{i=1}^{k} n_i c_i^0$$

$$A^1 = \sum_{i=1}^{k} n_i a_i^1 B^1 = \sum_{i=1}^{k} n_i b_i^1 C^1 = \sum_{i=1}^{k} n_i c_i^1 \tag{5}$$

where k is the number of all groups involved in the IL-ABS and n_i is the number of occurrences of group i. The group contributions a_i^0, b_i^0, c_i^0, a_i^1, b_i^1 and c_i^1 are generated by correlating the experimental binodal data points into Eq. (1).

For the first of all, each of the involved IL-ABS are, separately, correlated using Eq. (1). The resulting mean absolute error (MAE) of the correlation is 0.0086 with a squared correlation coefficient (R^2) of 0.9849, showing that the IL-ABS can be described well by this three-parameter model. The comparison between the experimental and Eq. (1)-calculated weight fraction of IL in ABS is presented in Fig. 2 and the error between experimental value of IL weight fraction ($x_{IL}^{Exp.}$) and correlated value of IL weight fraction ($x_{IL}^{Cor.}$) in ABS from Eq. (1) is given in Fig. 3. For a better illustration of the correlation performance of this three-parameter equation, we also provide the histogram of the regression deviations, as shown in Fig. 4. The obtained parameters (A^0, A^1, B^0, B^1, C^0, C^1) of all studied IL-ABS are provided in Table S3 (see Supporting Information). Some calculation examples of Eqs. (1)–(4) using these parameters are presented in Figs. 9–12. Although Eqs. (1)–(4) with these obtained parameters are able to provide reliable correlations, they are limited to a single IL-ABS. It means that different IL-based ABS have their own correlation coefficients, and they cannot be used interchangeably. Thus, it's impossible to use them to predict the phase equilibria behavior of those experimental data unavailable IL-ABS. In fact, the number of all reported IL-ABS is very small when compared to that of the possible existing IL-ABS, and some of them may have great potential in many specific applications. Therefore, a mathematical description with same coefficients that is capable to describe all IL-based ABS is highly desirable due to the fact it can provide quantitative information of structure–property for the optimal design of IL-based ABS. On the other hand, the introduction of GC methods would significantly improve the design space of IL-ABS, which means that we have more opportunities to find suitable IL-ABS with desired properties. For this purpose, we try to use GC-based method to simultaneously regress all involved IL-ABS. Unfortunately, the proposed GC-based linear model (with a MAE of 0.4827) fails to describe the phase composition of IL-ABS.

4. Nonlinear GC model

ANN inspired by biological neural systems, currently, are widely used in many technical fields due to their simplicity, flexibility and ability in the modeling systems (Sedghamiz et al., 2015; Lashkarbolooki et al., 2011). It is characterized by layered architec-

Table 1
Various IL-ABS with different phase -forming agent(s) involved in this work.

Ionic liquid	The second phase-forming agent
[C = C_2mIm][Cl]	D-sucrose (Wu et al., 2008)
[C = CmIm][Cl]	K_2L-tartrate, (Liu et al., 2016) K_3TO_7 (Liu et al., 2016)
[C_2mIm][BF_4]	$(NH_4)_2$DDS, (Han et al., 2011) $(NH_4)_2SO_4$, (Tang et al., 2014; Wu et al., 2018) Li_2SO_4; (Wang et al., 2013) $MgSO_4$; (Wang et al., 2013) Na_2HPO_4; (Lv et al., 2013) Na_2SO_3; (Yu et al., 2011) Na_2succinate, (Han et al., 2012) Na_3PO_4 (Yu et al., 2011), Na_3TO_7, (Han et al., 2012) $NaCH_3COO$, (Wu et al., 2018) NaH_2PO_4; (Wu et al., 2018; Lv et al., 2013) $ZnSO_4$ (Wang et al., 2013)
[C_2mIm][C_6SO_3]	K_3PO_4, (Patinha et al., 2013)
[C_2mIm][C_6SO_4]	$(NH_4)_2SO_4$, (Deive et al., 2011) K_2CO_3; (Deive et al., 2011) K_3PO_4; (Deive et al., 2011) Na_2CO_3 (Deive et al., 2011)
[C_2mIm][C_8SO_4]	$(NH_4)_2SO_4$, (Deive et al., 2011) Na_2CO_3 (Deive et al., 2011)
[C_2mIm][Cl]	K_2CO_3, (Zafarani-Moattar and Sarmad, 2011; Vargas et al., 2019) KH_2PO_4 (Ventura et al., 2011)
[C_2mIm][DMP]	K_2CO_3, (Wang et al., 2012) K_3PO_4 (Wang et al., 2012)
[C_2mIm][N(CN)$_2$]	K_3TO_7, (Gómez et al., 2018) Na_3TO_7 (Gómez et al., 2018)
[C_2mIm][Tf_2N]	nitric acid (Fu et al., 2016)
[C_2mPyr][CF_3COO]	K_3PO_4 (João et al., 2017)
[C_2Py][BF_4]	$(NH_4)_2SO_4$, (Li et al., 2014) $(NH_4)_3TO_7$, (Li et al., 2012, 2016) Na_2CO_3; (Li et al., 2014) Na_2succinate, (Li et al., 2012, 2016) Na_3TO_7 (Li et al., 2012)
[C_2Py][Br]	K_2PO_4, (Li et al., 2013) Na_2PHO_4; (Rogers and Seddon, 2003; Li et al., 2013) Na_2SO_4; (Li et al., 2013) NaH_2PO_4; (Li et al., 2013) NaKDDB (Li et al., 2013)
[C_3mIm][BF_4]	D-glucose, (Chen and Zhang, 2010) $(NH_4)_2$DDS, (Han et al., 2011) $(NH_4)_2SO_4$, (Tang et al., 2014; Wu et al., 2018) Na_2L-tartrate, (Wu et al., 2018) Na_2SO_3; (Yu et al., 2011) Na_2succinate, (Han et al., 2012) Na_3PO_4; (Yu et al., 2011) Na_3TO_7; (Wu et al., 2018) NaH_2PO_4 (Wu et al., 2018; Yu et al., 2011)
[C_3mIm][N(CN)$_2$]	K_3TO_7 (Gómez et al., 2018)
[C_4mIm][BF_4]	(Na)HCOO, (Gao et al., 2015) $(NH_4)_2$DDS, (Han et al., 2011) $(NH_4)_2SO_4$, (Tang et al., 2014; Wu et al., 2018; Wang et al., 2010) $(NH_4)_3TO_7$, (Wu et al., 2018; Han et al., 2010) $MgCl_2$; (Wang et al., 2016) $CuSO_4$; (Bonifácio, P.L.c., Aguiar, C.n.d.D., Alvarenga, B.G., Teixeira Lemes, N.H., Virtuoso, L.S., 2019) D-fructose, (Ventura, 2017; Jamehbozorg and Sadeghi, 2018; Zhang et al., 2007) D-glucose, (Chen and Zhang, 2010; Jamehbozorg and Sadeghi, 2018) D-maltose, (Jamehbozorg and Sadeghi, 2018; Chen et al., 2010) D-sucrose, (Wu et al., 2008; Jamehbozorg and Sadeghi, 2018; Chen et al., 2010) Li_2SO_4; (Wang et al., 2013) L-serine, (Zhang et al., 2007)] $MnSO_4$; (Alvarenga et al., 2013) Na_2CO_3; (Wu et al., 2018; Wang et al., 2010; Li et al., 2010) Na_2HPO_4; (Lv et al., 2012) Na_2L-tartrate, (Wu et al., 2018; Gao et al., 2015; Han et al., 2010) Na_2succinate, (Gao et al., 2015) Na_2WO_4; (Plechkova and Seddon, 2007; Wang et al., 2016) Na_3TO_7; (Gao et al., 2015; Han et al., 2010a, 2010b) $NaCH_3COO$, (Gao et al., 2015; Han et al., 2010) NaH_2PO_4; (Wu et al., 2018; Wang et al., 2010; Li et al., 2010) NaPHH, (Gao et al., 2015) $NiSO_4$; (das Dores Aguiar, C., Machado, P.A.L., Alvarenga, B. G., Lemes, N.H.T., Virtuoso, L.S., 2017)] $ZnSO_4$ (Wang et al., 2013; das Dores Aguiar et al., 2017)
[C_4mIm][Br]	Cs_2SO_4, (Li et al., 2019) HK_2PO_4; (Mourão et al., 2012; Pei et al., 2007; Zafarani-Moattar and Hamzehzadeh, 2007) K_3TO_7; (Zafarani-Moattar and Hamzehzadeh, 2009) Na_3TO_7 (Zafarani-Moattar and Hamzehzadeh, 2010; Sadeghi et al., 2010)
[C_4mIm][CF_3SO_3]	2a-acid, (Noshadi and Sadeghi, 2017) KCH_3COO, (Quental et al., 2015) L-serine, (Noshadi and Sadeghi, 2017) Na_2L-tartrate, (Liu and Jin, 2016; Gao et al., 2015) Na_2succinate, (Gao et al., 2015) Na_3TO_7; (Gao et al., 2015) NaC_2H_5COO, (Gao et al., 2015) $NaCH_3COO$, (Gao et al., 2015; Quental et al., 2015) NaH_2PO_4; (Alvarez-Guerra et al., 2014) NaHCOO, (Quental et al., 2015) NaPHH (Vekariya, 2017; Gao et al., 2015)
[C_4mIm][Cl]	K_2CO_3, (Zafarani-Moattar and Hamzehzadeh, 2010) K_3PO_4; (Gao et al., 2014) K_3TO_7; (Zafarani-Moattar and Hamzehzadeh, 2010) KH_2PO_4 (Ventura et al., 2011)
[C_4mIm][DMP]	HK_2PO_4 (Wang et al., 2012)
[C_4mIm][N(CN)$_2$]	(Na)HCOO, (Gao et al., 2015) HK_2PO_4; (Mourão et al., 2012) K_3TO_7; (Gómez et al., 2018) Na_2L-tartrate, (Gao et al., 2015) Na_3TO_7 (Gómez et al., 2018)
[C_4mim][NO_3]	HK_2PO_4, (Malekghasemi et al., 2016) K_2CO_3 (Malekghasemi et al., 2016)
[C_4mIm][Tos]	HK_2PO_4, (Mourão et al., 2012) K_3PO_4 [104
[C_4mPy][BF_4]	$(NH_4)_2SO_4$, (Xu et al., 2019; Li et al., 2015) $(NH_4)_3TO_7$, (Li et al., 2013) Na_2HPO_4; (Li et al., 2015) Na_2L-tartrate, (Li et al., 2013) Na_2SO_4; (Li et al., 2015; Li and Wu, 2015) Na_3TO_7; (Li et al., 2013) NaH_2PO4 (Li et al., 2015; Li and Wu, 2015)
[C_4mPy][Br]	K_3PO4 (Dimitrijević et al., 2020)
[C_4mPy][CF_3SO_3]	D-fructose, (Okuniewski et al., 2016) D-glucose (Okuniewski et al., 2016)
[C_4mPyr][CF_3SO_3]	D-fructose, (Okuniewski et al., 2016) D-glucose, (Okuniewski et al., 2016) D-sorbitol, (Ventura, 2017; Okuniewski et al., 2016) xylitol (Okuniewski et al., 2016)
[C_4mPyr][N(CN)$_2$]	K_3TO_7, (Gómez et al., 2018) Na_3TO7 (Gómez et al., 2018)
[C_4Py][BF_4]	$(NH_4)_2SO_4$, (Li et al., 2014, 2016) $(NH_4)_3TO_7$, (Li et al., 2014, 2016) Na_2HPO_4; (Li et al., 2014) Na_2L-tartrate, (Li et al., 2013) Na_2SO_4; (Li et al., 2014, 2016) Na_2succinate, (Li et al., 2014) Na_3TO_7; (Li et al., 2014) $NaCH_3COO$, (Li et al., 2014, 2016) NaH_2PO4 (Li et al., 2016)
[C_4Py][CF_3SO_3]	$(NH_4)_2SO_4$, (Guo et al., 2020) $(NH_4)_3TO_7$, (Li et al., 2016) Na_2succinate, (Li et al., 2016) NaH_2PO4 (Guo et al., 2020)
[C_4Py][NO_3]	$(NH_4)_2SO4$, (Li et al., 2017) Na_2SO4 (Xu et al., 2019)
[C_5mIm][$MeSO_3$]	K_3PO4 (Patinha et al., 2013)
[C_6mIm][Br]	Cs_2SO4 (Li et al., 2019)
[C_6mIm][Cl]	Cs_2SO_4, (Li et al., 2019) HK_2PO_4; (Wu et al., 2018) K_2L-tartrate, (Han et al., 2014) K_3PO_4; (Gao et al., 2014) KH_2PO_4; 78] Na_2CO3 (Deive et al., 2011)
[C_6mIm][N(CN)$_2$]	K_3TO7 (Gómez et al., 2018)
[C_6mIm][NO_3]	HK_2PO_4, (Malekghasemi et al., 2016) K_2CO3 (Malekghasemi et al., 2016)
[C_8mIm][Br]	HK_2PO4 (Fang et al., 2018)
[C_8mIm][Cl]	Cs_2SO4 (Li et al., 2019)
[C_8mIm][NO_3]	HK_2PO_4, (Malekghasemi et al., 2016) K_2CO3 (Malekghasemi et al., 2016)
[N_{1112OH}][C_3COO]	K_2CO3 (Almeida et al., 2019)
[N_{1112OH}][C_4COO]	K_2CO3 (Almeida et al., 2019)
[N_{1112OH}][C_5COO]	K_2CO3 (Almeida et al., 2019)
[N_{1112OH}][C_6COO]	K_2CO3 (Almeida et al., 2019)
[N_{1112OH}] [glycinate]	HK_2PO4 (Gómez et al., 2019)
[N_{1112OH}][L-alaninate]	K_3PO4 (Gómez et al., 2019)
[N_{1112OH}][L-serinate]	HK_2PO4 (Gómez et al., 2019)
[N_{2222}][Cl]	K_2CO3 (Sintra et al., 2014)
[N_{3333}][Br]	K_2CO3 (Sintra et al., 2014)
[N_{3333}][Cl]	K_2CO3 (Sintra et al., 2014)
[N_{4444}][C_3COO]	K_3PO4 (Basaiahgari and Gardas, 2018)

Table 1 (*continued*)

Ionic liquid	The second phase-forming agent
[N_{4444}][Cl]	K_2CO3 (Sintra et al., 2014)
[Nbis][STP]	HK_2PO_4, (Yao et al., 2017) K_2CO_3; (Yao et al., 2017) K_3PO_4; (Yao et al., 2017) Na_2CO3 (Yao et al., 2017)
[P_{1333}][Tos]	K_2CO3 (Sintra et al., 2014)
[P_{1444}][$MeSO_4$]	K_2CO3 (Sintra et al., 2014)
[P_{4444}][Br]	K_2CO3 (Sintra et al., 2014)
[P_{4444}][Cl]	K_2CO3 (Sintra et al., 2014)
[P_{4448}][Br]	K_3PO4 (Gao et al., 2017)

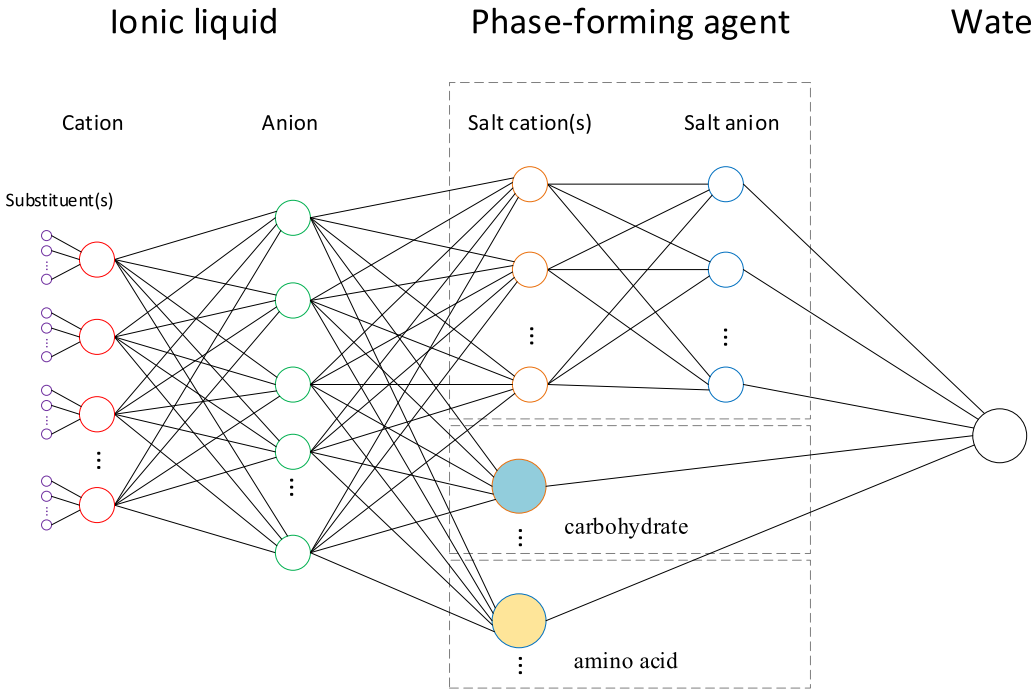

Fig. 1. Structure of IL-ABS described by building blocks from the concept of GC method.

tures and feed-forward connections between neurons, or back connections. Weights are assigned to these connections between the neurons of one layer and the next. The benefits of using ANN can be summarized as: (i) ANN can learn organically. This means their outputs aren't limited entirely by inputs and they have the ability to generalize their inputs; (ii) nonlinear systems have the capability of finding shortcuts to reach computationally expensive solutions; (iii) ANN have the potential for high fault tolerance; (iv) ANN can do more than routing around parts of the network that no longer operate. (https://www.allerin.com/blog/4-benefits-of-using-artificial-neural-nets) The advantages of ANN are highlighted when a large experimental data in the wide ranges of variables is available. To date, a series of ANN-based nonlinear GC models have been developed for the prediction of various properties and results show that they are able to provide better performance than linear models (Zhao et al., 2014; Peng and Picchioni, 2020). For this reason, here we try to use ANN for building a nonlinear GC model to describe the phase properties of IL-ABS. In this work, a popular ANN architecture that comprises of a three-layer feed forward network is used (see Fig. 5). The input layer reads the structure information of IL and the second phase-forming agent involved in IL-ABS (denoted as 71 group numbers) and the weight fraction of IL and the second phase-forming agent and the temperature, which totally giving an input vector with a size of 73 × 1. The hidden layer transfers and delivers this input information to the output layer where the phase composition of IL-ABS is estimated, and the summation of errors between experimental and model-estimated weight fractions of IL are quantified. For a given input vector p, the output from the hidden layer $f_1(a_1)$ is calculated by Eq. (6) and the output of the output layer $f_2(a_2)$ is determined by Eq. (7).

$$f_1(a_1) = f_1(W_1 \times P + b_1) \tag{6}$$

$$f_2(a_2) = f_2(W_2 \times f_1(a_1) + b_2) \tag{7}$$

As reported, (Song et al., 2020) combining the application of tansig transfer function (see Eq. (8)) in the hidden layer with the application of purelin transfer function (see Eq. (9)) in the output layer is a very effective way to build a three-layer neural network in MATLAB. For this reason, such a combination is also employed to build the ANN-GC model in this work.

$$f_1(x) = \frac{2}{1 + e^{-2x}} - 1 \tag{8}$$

$$f_2(x) = x \tag{9}$$

In ANN, selecting a suitable number of neurons in the hidden layer is essential due to the network with too few neurons may not be powerful enough for achieving good predictions, while the network with too large number of neurons tends to perform over-fitting. Typically, this number is specified before the regression of the weight matrices (W_1, W_2) and bias vectors (b_1, b_2). In order to identify the number of neurons in the hidden layer, we train the ANN-GC model with a series of neurons in the hidden

Table 2
Building groups decomposed from all involved ILs and the second phase-forming agents.

ILs		The second phase-forming agents	
Names	Abbreviations	Names	Abbreviations
Cations		**Salt cations**	
imidazolium	[Im]	sodium	Na
pyridinium	[Py]	potassium	K
pyrrolidinium	[Pyr]	ammonium	NH_4
ammonium	[N]	hydrogen	H
phosphonium	[P]	caesium	Cs
N-(bis(dimethylamino)methylene)ethanaminium	[Nbis]	magnesium	Mg
Anions		nickel	Ni
bis((trifluoromethyl)sulfonyl)imide	[Tf_2N]	lithium	Li
tetrafluoroborate	[BF_4]	copper	Cu
chloride	[Cl]	manganese	Mn
bromide	[Br]	zinc	Zn
butanoate	[C_3COO]	**Salt anions**	
penanoate	[C_4COO]	2-hydroxypropane-1,2,3-tricarboxylate	TO_7
hexanoate	[C_5COO]	dihydrogen phosphate	H_2PO_4
hepanoate	[C_6COO]	hydrogen phosphate	HPO_4
methyl sulfate	[$MeSO_4$]	phosphate	PO_4
hexyl sulfate	[C_6SO_4]	sulfate	SO_4
octyl sulfate	[C_8SO_4]	carbonate	CO_3
trifluoromethanesulfonate	[CF_3SO_3]	ethanoate	CH_3COO
trifluoroacetate	[CF_3COO]	propanoate	C_2H_5COO
methanesulfonate	[$MeSO_3$]	sulfite	SO_3
hexanesulfonate	[C_6SO_3]	tungstate	WO_4
dimethylphosphate	[DMP]	methanoate	HCOO
dicyanamide	[$N(CN)_2$]	meso-tartrate	meso-tartrate
nitrate	[NO_3]	succinate	succinate
tosylate	[Tos]	L-tartrate	L-tartrate
4-sulfonatooxy-2,2,6,6-tetramethylpiperidine-1-yloxyl	[STP]	(2R,3R)-2,3-dihydroxysuccinate	DDS
L-alaninate	L-alaninate	(2R,3R)-2,3-dihydroxybutanedioate	DDB
L-serinate	L-serinate	(2R,3S,4R,5R)-2,3,4,5,6-pentahydroxyhexanoate	PHH
glycinate	glycinate	**Carbohydrates**	
Substituents		D-glucose	D-glucose
methyl	$-CH_3$	D-maltose	D-maltose
methylene	$-CH_2-$	D-sucrose	D-sucrose
hydroxy	−OH	D-fructose	D-fructose
vinyl	$-CH=CH_2-$	D-sorbitol	D-sorbitol
hydrogen	−H	xylitol	xylitol
		Amino acids	
		L-serine	L-serine
		2-aminoacetic acid	2a-acid
		nitric acid	N-acid

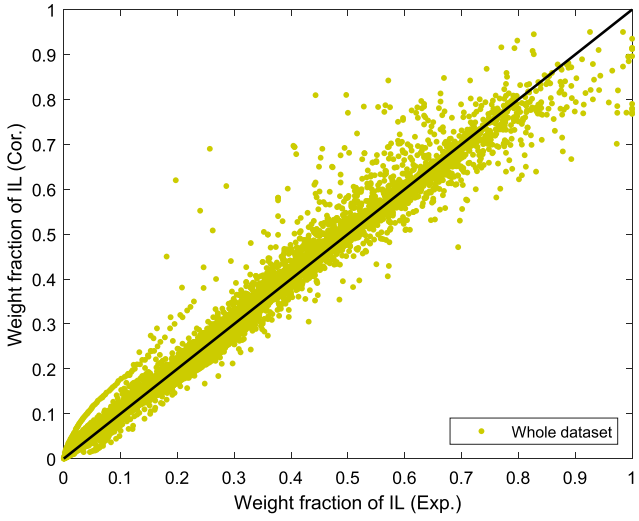

Fig. 2. Comparison between the experimental and Eq. (1)-calculated weight fraction of IL in ABS.

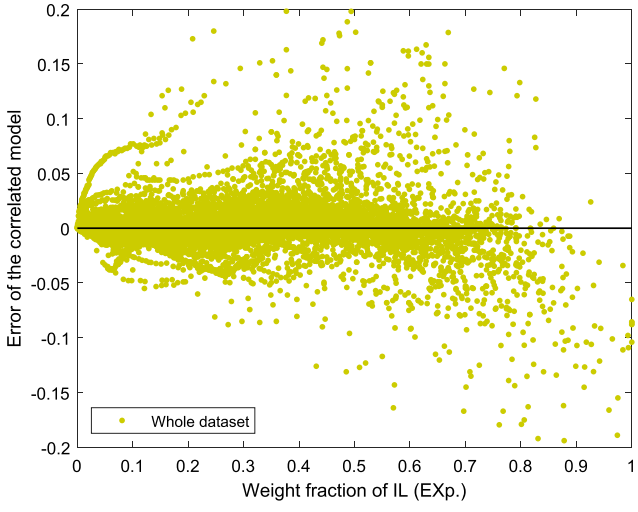

Fig. 3. Error ($x_{IL}^{Exp.} - x_{IL}^{Cor.}$) of Eq. (1) for correlating the weight fraction of IL in ABS.

layer. Finally, the network with 2 neurones in the hidden layer is identified has the best performance. Based on this number of neurons, weight and bias parameters are optimized using the Levenberg-Marquardt algorithm (in MATLAB), in which the minimization of the summation of absolute errors between the experimental and model-predicted weight fraction of IL in the training dataset is taken as the objective function. The values of W_1,W_2, b_1, and b_2 are given in the Supporting Information.

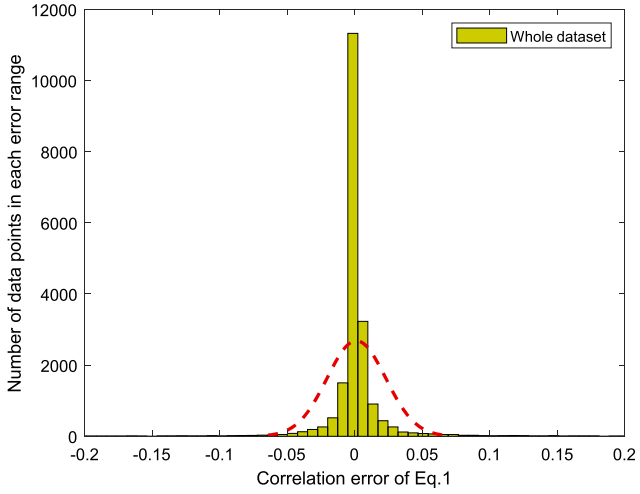

Fig. 4. Distribution of the correlation error of Eq. (1).

This nonlinear GC model gives a MAE of 0.0175 and R^2 of 0.9316 for the 13,789 training data points, and for the 3,660 test data points they are 0.0177 and 0.9195, respectively. The comparison between the experimental and model-predicted weight fraction of the second phase-forming agent for both training set and test set are presented in Fig. 6. Meanwhile, Fig. 7 gives the errors between the experimental ($x_{agent}^{Exp.}$) and model-predicted ($x_{agent}^{Pre.}$) weight fraction of the second phase-forming agent. For a better illustration of the model performance, we also provide the histogram of the prediction deviations, as shown in Fig. 8. In general, the proposed ANN-GC model is able to describe phase composition of various IL-ABS at different temperature. An example of using this nonlinear ANN-GC model to predict the ternary phase diagram of three different IL-ABS is provided in Appendix.

5. Results and discussions

From Figs. 1 and 2, it is clear that Eq. (1) can well describe each of the IL-ABS at different temperatures. However, on the other hand, the linear GC model based on this three-parameter mathematical description is unable to simultaneously represent the phase property of IL-ABS. This can be explained by the complexity of these biphasic systems. On the other hand, the proposed nonlinear ANN-GC model provides acceptable MAE and R^2 for both training set (0.0173, 0.9316) and test set (0.0177, 0.9195). Among all predictions from this nonlinear ANN-GC model, most of them have small deviations (close to zero) and only a very limited number of them have absolute errors higher than 0.1 which may be attributed to experimental deviations among different measurements, as shown in Fig. 8. Despite the developed ANN-GC model is able to provide reliable predictions, we should not ignore that unlike the traditional models such as UNIFAC and NRTL, this ANN-GC model

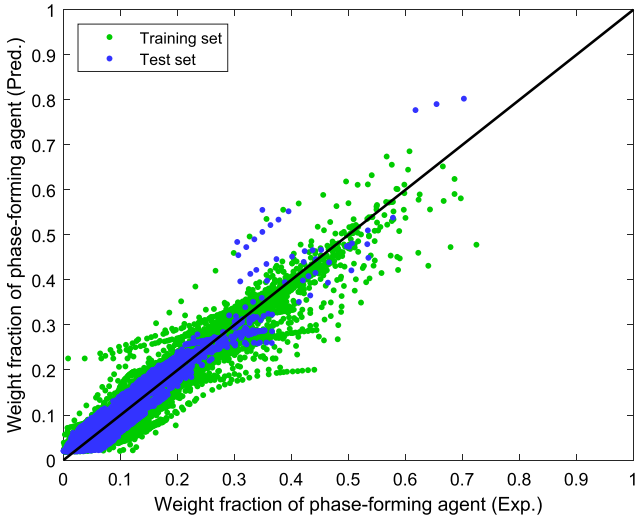

Fig. 6. Comparison between the experimental and model-predicted weight fraction of the second phase-forming agent in ABS.

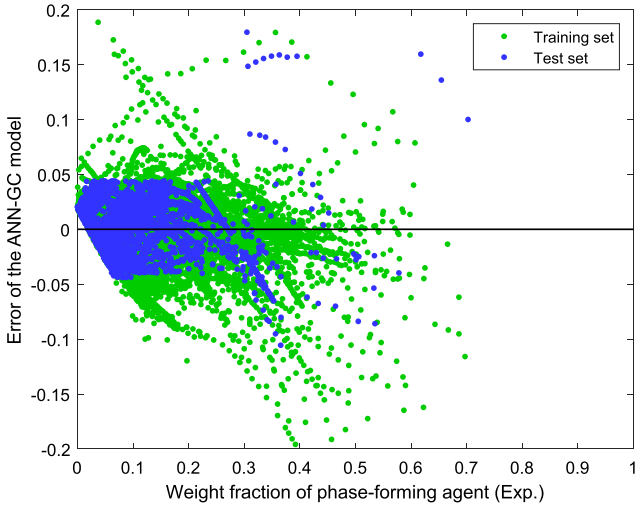

Fig. 7. Error ($x_{agent}^{Exp.} - x_{agent}^{Pre.}$) of the nonlinear GC model for predicting the weight fraction of the second phase-forming agent in ABS.

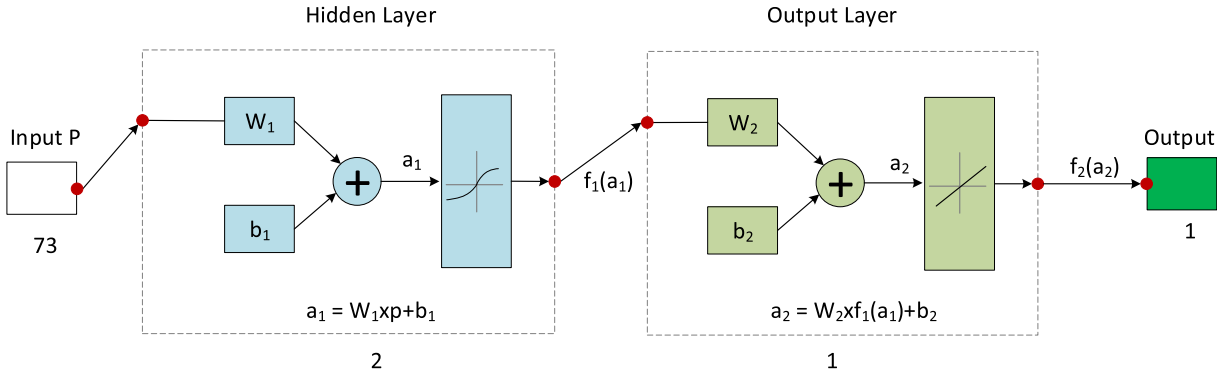

Fig. 5. Structure of the three-layer artificial neural network (ANN) with 2 neurons in the hidden layer.

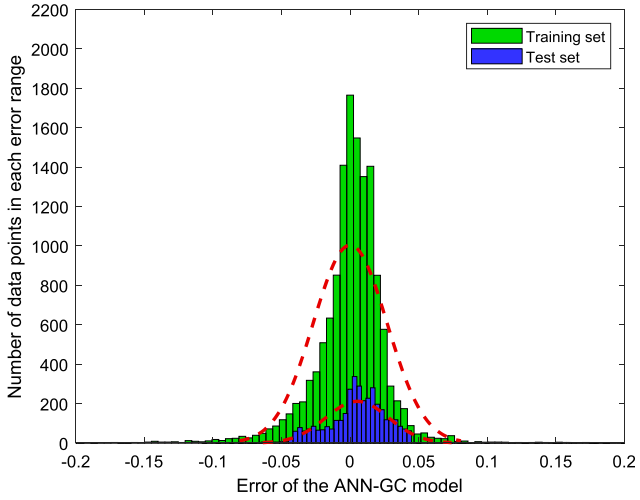

Fig. 8. Distribution of the prediction error of the nonlinear GC model.

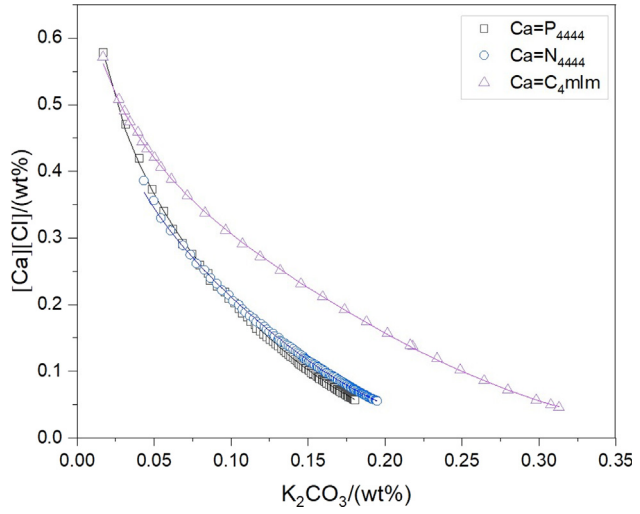

Fig. 9. Ternary phase diagrams for ABS composed of chloride-based ILs + K_2CO_3 +- H_2O at room temperature. Symbols are experimental data (Zafarani-Moattar and Hamzehzadeh, 2010; Sintra et al., 2014) and lines are calculated values from Eqs.1–4 using the parameters obtained in this work.

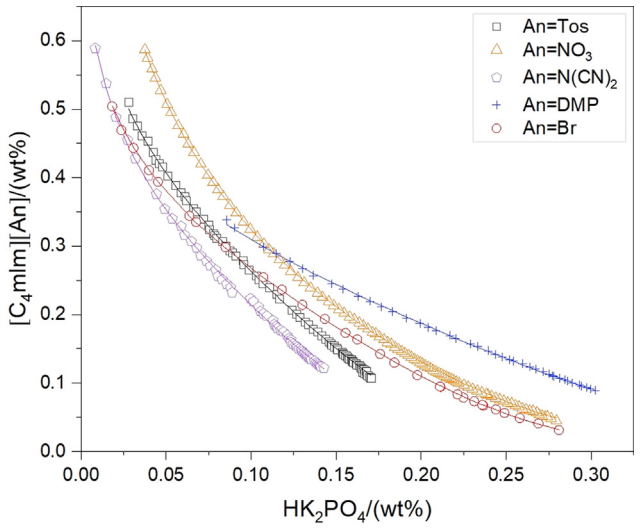

Fig. 10. Ternary phase diagrams for ABS composed of [C_4mIm]-based ILs + K_2HPO_4 +- H_2O at room temperature. Symbols are experimental data(Wang et al., 2012; Mourão et al., 2012; Malekghasemi et al., 2016) and lines are calculated values from Eqs. (1)–(4) using the parameters obtained in this work.

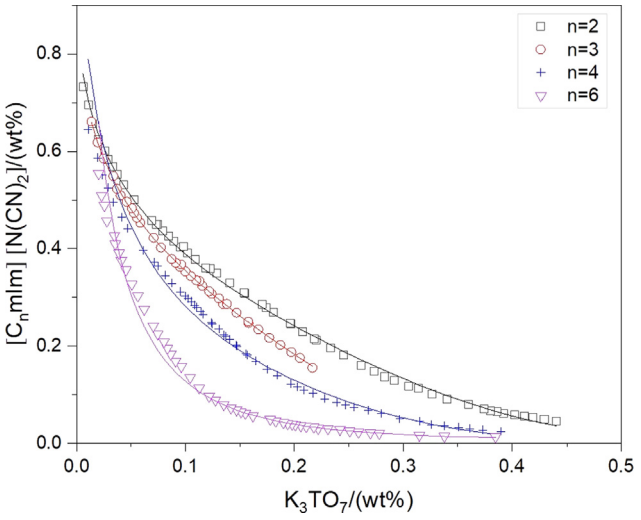

Fig. 11. Ternary phase diagrams for ABS composed of [C_nmIm][$N(CN)_2$] + K_3TO_7 +- H_2O at room temperature (n = 2,3,4,6). Symbols are experimental data (Gómez et al., 2018) and lines are calculated values from Eqs. (1)–(4) using the parameters obtained in this work.

is not derived from thermodynamic principles. Therefore, we use it as a predictive tool/model rather than a thermodynamic model.

Besides the efforts of building linear/nonlinear GC model to describe the phase property of IL-ABS, we also investigate the influence of IL and the second phase-forming agent on the phase formation of IL-ABS from the group level. As we know, the closer to the axis origin a binodal curve is, the greater is the ability of an IL to phase split. Fig. 9 indicates that the ability of IL with different cations to form ABS in the presence of K_2CO_3, follow the order: $[P_{4444}][Cl] \geq [N_{4444}][Cl] > [C_4mIm][Cl]$. Similar trend has also been observed when using other salts (e.g., K_3PO_4, K_2HPO_4) as the second phase-forming agent. (Bridges et al., 2007; Louros et al., 2010) This is due to the phosphonium/ammonium-based ILs have highly shielded charges and mostly located on the heteroatom surrounded by four alkyl chains, which results in a higher tendency toward salting out from water solution. (Bridges et al., 2007) Similarly, the charge of a pyridinium-based IL mostly locates on the nitrogen atom, but it generally has less shielding when compared to the phosphonium /ammonium-based ILs. In contrast, the charge of an imidazolium-based IL disperses evenly along the entire heterocycle, and this cation can also interact with water through hydrogen-bonding. (Freire et al., 2012) As the other ion in IL, the anion also has influence on the ability of the IL to produce ABS. As reported, the ability of an IL anion to form ABS generally follows the decrease in their hydrogen-bond accepting strength or electron pair donation ability. (Ventura et al., 2009) Fig. 10 presents the experimental phase diagrams of water-K_2HPO_4-IL with different anions; it reveals that in the region with low salt concentration, the ability of the anions to form ABS increases in the order: [N $(CN)_2$] ≥ [Br] > [Tos] ≥ [DMP] > [NO3]. For the region with high salt concentration, the order is [$N(CN)_2$] > [Tos] > [Br] > [NO3] > [DMP].

Similar to many other properties such as viscosity, toxicity of ILs, the cation alkyl chain length also has big influence on the phase behaviour of IL-based ABS. Generally, the hydrophobicity of an IL increases with the increase of the cation alkyl chain length, and therefore ILs with longer cation alkyl side chain tends to have less

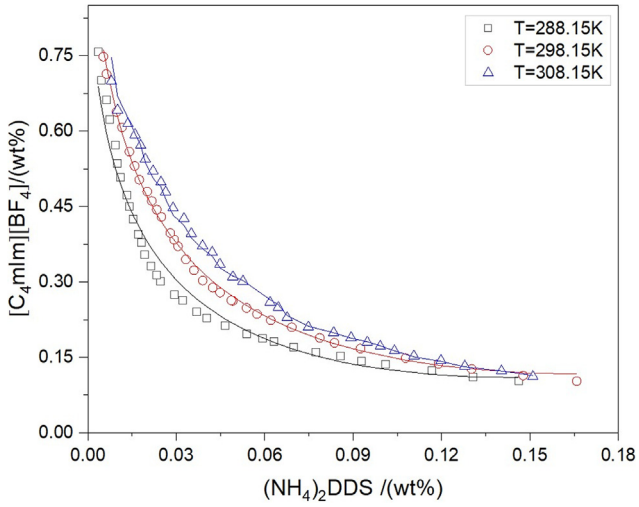

Fig. 12. Ternary phase diagrams for ABS composed of $[C_4mIm][BF_4]$ + $(NH_4)_2$-DDS + H_2O at different temperatures (T = 288.15 K, 298.15 K, 308.15 K). Symbols are experimental data (Han et al., 2011) and lines are calculated values from Eqs. (1)–(4) using the parameters obtained in this work.

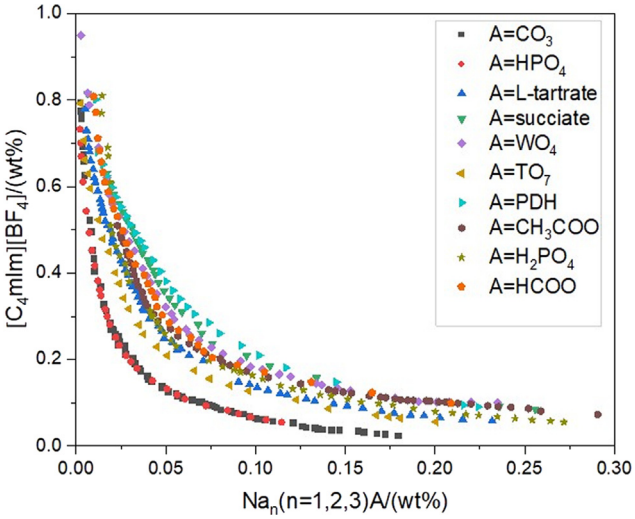

Fig. 13. Ternary phase diagrams for ABS composed of sodium-based salts + $[C_4mIm][BF_4]$ + H_2O at room temperature. (Wu et al., 2018; Gao et al., 2015; Wang et al., 2016).

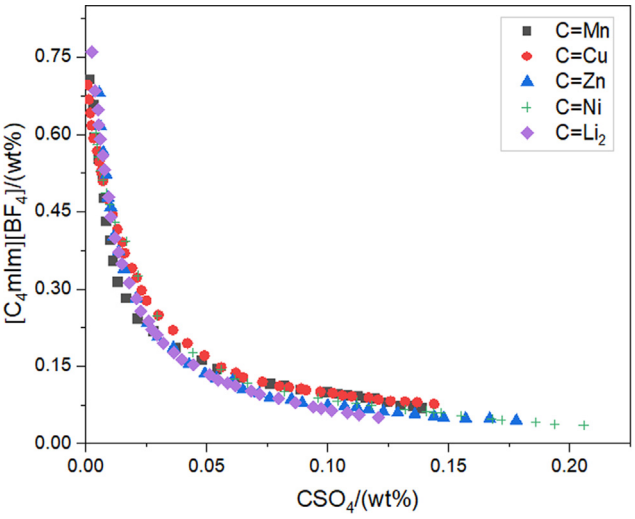

Fig. 14. Ternary phase diagrams for ABS composed of sulfate-based salts + $[C_4mIm][BF_4]$ + H_2O at room temperature. (Wang et al., 2013; Bonifácio et al., 2019; Alvarenga et al., 2013; das Dores Aguiar et al., 2017).

solubility in water. For this reason, ILs with longer cation alkyl side chain require less salt for salting-out and are more easily excluded from the salt-rich phase to the ionic-liquid-rich phase. (Freire et al., 2012) It means that the ability of the ILs to form ABS generally increases with the increase in cation alkyl chain length, an example of this trend is presented in Fig. 11. It is to be noted that this trend only works under a certain number of the cation alkyl chain (e.g., hexyl, octyl) due to the ABS may not exist when the cation alkyl chain of the ILs is too long. On the other side, temperature also plays an important role on the creation of ABS containing IL. Fig. 12 gives an example of the influence from temperature on the phase diagrams of ionic-liquid-based ABS. Obviously, the lower the temperature, the less the IL and salting-out agent are required for the phase split. This phenomenon has also been observed by other authors and it can be attributed to the fact that the interaction between the IL and water increases with the increase of temperature, and therefore improving their mutual solubilities (Zafarani-Moattar and Hamzehzadeh, 2009, 2010; Wang et al., 2010; Sadeghi et al., 2010). However, it should be noted that temperature has no major influence on the phase separation of some aqueous systems containing IL. Nonetheless, lower temperatures are favourable to induce the formation of IL-ABS is a general agreement (Freire et al., 2012).

Besides the influences of the cation and anion of the IL, and the temperature on the formation of ABS, the effect of the second phase-forming agent also needs to be taken into accounted in the preparation of IL-ABS. Currently, most studied IL-ABS use conventional salt as the second phase-forming agent, a few of them involving amino acids and carbohydrates. The amount of salt required to produce ABS largely depends on the salting-out strength of the salt. Fig. 13 gives an example of the salt anion influence on the creation of IL-ABS, while the salt cation influence is presented as another example (see Fig. 14). As reported, (Freire et al., 2012) salt anions with higher valence have higher salting-out ability than those with lower one because the latter are more hydrated. However, the binodal curves shown in Fig. 13 indicate that salt anions in some IL-ABS do not follow this rule. On the other hand, it seems that the salt cation has little influence on the phase split in IL-ABS. However, salts with different cations exhibit different salting-out capabilities in some other IL-ABS (Shill et al., 2011). In conclusion, there is no general rule to guide the salt cation and anion influence on the formation of ABS, and they need to be carefully evaluated in the preparation of ABS with different ILs. Nonetheless, the salting-out in IL-ABS is an entropically driven process, as the idea proposed for hydrophobic ionic liquids and a wide range of salts (Tomé et al., 2009; Freire et al., 2010).

6. Conclusion

The ionic liquid database developed in our previous work has been extended to IL-based aqueous biphasic systems. In total, 17,449 experimental binodal data points covering 171 IL-ABS at different temperatures (278.15 K–343.15 K) are collected. All involved IL-ABS are correlated using a popular three-parameter mathematical description and the optimal parameters of each IL-ABS are obtained. Based on this mathematical description, we try to build a linear GC model to predict the phase equilibria behavior of IL-ABS, but it fails due to the high complexity of these biphasic systems. On the other hand, the proposed nonlinear ANN-GC model gives a MAE of 0.0175 and R^2 of 0.9316 for the 13,789 train-

ing data points, and for the 3,660 test data points they are 0.0177 and 0.9195, respectively. The results suggest that this nonlinear GC model, to some extent, can give reliable predictions on the phase equilibria behavior of IL-ABS. This model provides the possibility of using computer-aided design method in the optimal design of IL-ABS, which would significantly improve the opportunity of finding optimal IL-ABS for specific tasks.

Besides the efforts of building GC models, we also discuss some main issues that govern the phase equilibria behavior of IL-ABS. The quaternary phosphonium/ammonium-based ILs have higher ability to create ABS than that of pyridinium and imidazolium-based ILs, while the ability of an IL anion to form ABS generally follows the decrease in their hydrogen-bond accepting strength or electron pair donation ability. On the other hand, the ability of an IL to produce ABS generally increases with the increase in cation alkyl chain length and lower temperatures are favorable to induce the formation of IL-ABS is a general agreement, although temperature has no major influence on the phase split of some IL-ABS. In addition, salt anions with higher valence are reported have higher salting-out ability than those with lower one because the latter are more hydrated, but some IL-ABS do not follow this rule. Meanwhile, salts with different cations exhibit different salting-out capabilities in different IL-ABS. Therefore, there is no general rule to guide the salt cation and anion influence on the formation of ABS, and they need to be carefully evaluated in the preparation of ABS with different ILs. All conclusions mentioned above could be a guidance in the design of IL-ABS.

CRediT authorship contribution statement

Yuqiu Chen: Conceptualization, Methodology, Software, Investigation, Writing - original draft. **Xiaodong Liang:** Project administration, Writing - review & editing. **John M. Woodley:** Supervision, Writing - review & editing. **Georgios M. Kontogeorgis:** Supervision, Writing - review & editing, Resources.

Declaration of Competing Interest

The authors declare that they have no known competing financial interests or personal relationships that could have appeared to influence the work reported in this paper.

Acknowledgement

This research work was supported by the China Scholarship Council (No. 201708440264) and the Technical University of Denmark.

Appendix A

Here we provide an example of using the developed nonlinear ANN-GC model to predict the ternary phase diagram of three different IL-ABS, i.e. [N_{4444}][Cl] + K_2CO_3 + H_2O at 298.00 K, [C_4mIm][Cl] + K_2CO_3 + H_2O at 298.15 K, and [C_4Py][BF_4]+$(NH_4)_2SO_4$ + H_2O at 308.15 K. Weight fraction of the second phase-forming agent can be calculated as following:

$$x_{agent}/wt\% = W_2 \cdot \left(\frac{2}{1+e^{-2(W_1 \cdot p + b_1)}} - 1\right) + b_2$$

The vector p and the mode parameters (W_1, b_1, W_2, b_2) can be found in Table S6 (Supporting Information). Fig. A1 gives the comparison between the experimental and ANN-GC model predicted ternary phase diagram of the exemplified IL-ABS systems.

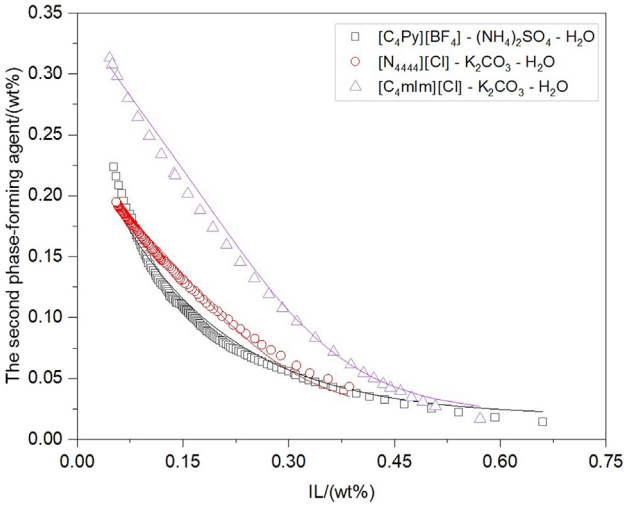

Fig. A1. Comparison between the experimental and ANN-GC model predicted ternary phase diagram composed of the exemplified IL-ABS systems. (Zafarani-Moattar and Hamzehzadeh, 2010; Li et al., 2016; Sintra et al., 2014).

Appendix B. Supplementary material

Supplementary data to this article can be found online at https://doi.org/10.1016/j.ces.2021.116904.

References

Absalan, G., Akhond, M., Sheikhian, L., 2008. Extraction and high performance liquid chromatographic determination of 3-indole butyric acid in pea plants by using imidazolium-based ionic liquids as extractant. Talanta 77, 407–411.
Absalan, G., Akhond, M., Sheikhian, L., 2010. Partitioning of acidic, basic and neutral amino acids into imidazolium-based ionic liquids. Amino Acids 39, 167–174.
Almeida, M.R., Belchior, D.C., Carvalho, P.J., Freire, M.G., 2019. Liquid-liquid equilibrium and extraction performance of aqueous biphasic systems composed of water, cholinium carboxylate ionic liquids and K2CO3. J. Chem. Eng. Data 64, 4946–4955.
Alshehri, A.S., Gani, R., You, F., 2020. Deep learning and knowledge-based methods for computer-aided molecular design—toward a unified approach: state-of-the-art and future directions. Comput. Chem. Eng. 107005.
Alvarenga, B.G., Virtuoso, L.S., Lemes, N.H.T., Luccas, P.O., 2013. Phase behaviour at different temperatures of an aqueous two-phase ionic liquid containing ([Bmim] BF4+ manganese sulfate+ water). J. Chem. Thermodyn. 61, 45–50.
Alvarez-Guerra, E., Ventura, S.P., Coutinho, J.A., Irabien, A., 2014. Ionic liquid-based three phase partitioning (ILTPP) systems: Ionic liquid recovery and recycling. Fluid Phase Equilib. 371, 67–74.
Asenjo, J.A., Andrews, B.A., 2012. Aqueous two-phase systems for protein separation: phase separation and applications. J. Chromatogr. A 1238, 1–10.
Basaiahgari, A., Gardas, R.L., 2018. Evaluation of anion chain length impact on aqueous two phase systems formed by carboxylate anion functionalized ionic liquids. J. Chem. Thermodyn. 120, 88–96.
Bi, W., Zhou, J., Row, K.H., 2012. Solid phase extraction of three phenolic acids from Saliconia herbacea L. by different ionic liquid-based silicas. J. Liq. Chromatogr. Relat. Technol. 35, 723–736.
Bonifácio, P.L.c., Aguiar, C.n.d.D., Alvarenga, B.G., Teixeira Lemes, N.H., Virtuoso, L.S., 2019. Phase Behavior in Aqueous Two-Phase Systems Based-Ionic Liquid Composed of 1-Butyl-3-methylimidazolium Tetrafluoroborate and Copper Sulfate in Different Temperatures. J. Chem. Eng. Data 64, 2143-2152.
Bridges, N.J., Gutowski, K.E., Rogers, R.D., 2007. Investigation of aqueous biphasic systems formed from solutions of chaotropic salts with kosmotropic salts (salt–salt ABS). Green Chem. 9, 177–183.
Cao, L., Zhu, P., Zhao, Y., Zhao, J., 2018. Using machine learning and quantum chemistry descriptors to predict the toxicity of ionic liquids. J. Hazard. Mater. 352, 17–26.
Chen, Y., Liu, X., Kontogeorgis, G.M., Woodley, J.M., 2020. Gas solubility in ionic liquids (ILs): UNIFAC-IL model extension. Ind. Eng. Chem. Res. Under review.
Chen, Y., Meng, Y., Zhang, S., Zhang, Y., Liu, X., Yang, J., 2010. Liquid– liquid equilibria of aqueous biphasic systems composed of 1-butyl-3-methyl imidazolium tetrafluoroborate+ sucrose/maltose+ water. J. Chem. Eng. Data 55, 3612–3616.
Chen, Y., Koumaditi, E., Woodley, J., Kontogeorgis, G., Gani, R., 2018. Integrated Solvent-Membrane and Process Design Method for Hybrid Reaction-Separation Schemes. Comput. Aided Chem. Eng.; Elsevier Vol. 43, 851–856.

Chen, Y., Woodley, J., Kontogeorgis, G., Gani, R., 2018. Integrated ionic liquid and process design involving hybrid separation schemes. Comput. Aided Chem. Eng.; Elsevier Vol. 44, 1045–1050.
Chen, Y., Gani, R., Kontogeorgis, G.M., Woodley, J.M., 2019. Integrated ionic liquid and process design involving azeotropic separation processes. Chem. Eng. Sci. 203, 402–414.
Chen, Y., Koumaditi, E., Gani, R., Kontogeorgis, G.M., Woodley, J.M., 2019. Computer-aided design of ionic liquids for hybrid process schemes. Comput. Chem. Eng. 130, 106556.
Chen, Y., Kontogeorgis, G.M., Woodley, J.M., 2019aa. Group contribution-based estimation method for properties of ionic liquids. Ind. Eng. Chem. Res.
Chen, Y., Cai, Y., Thomsen, K., Kontogeorgis, G.M., Woodley, J.M., 2020bb. A group contribution-based prediction method for the electrical conductivity of ionic liquids. Fluid Phase Equilib. 509, 112462.
Chen, Y., Zhang, S., 2010. Phase behavior of (1-alkyl-3-methyl imidazolium tetrafluoroborate+ 6-(hydroxymethyl) oxane-2, 3, 4, 5-tetrol+ water). J. Chem. Eng. Data 55, 278–282.
Chen, Y., Liu, X., Kontogeorgis, G.M., Woodley, J.M., 2020. Ionic-liquid-based bioisoprene recovery process design. Ind. Eng. Chem. Res. 59, 7355–7366.
das Dores Aguiar, C., Machado, P.A.L., Alvarenga, B.G., Lemes, N.H.T., Virtuoso, L.S., 2017. Phase behaviour at different temperatures of ionic liquid based aqueous two-phase systems containing {[Bmim] BF4+ salt sulfate (Zn2+ or Ni2+)+ water}. J. Chem. Thermodyn. 108, 105-117.
Deive, F.J., Rivas, M.A., Rodríguez, A., 2011. Sodium carbonate as phase promoter in aqueous solutions of imidazolium and pyridinium ionic liquids. J. Chem. Thermodyn. 43, 1153–1158.
Deive, F.J., Rodríguez, A., Marrucho, I.M., Rebelo, L.P., 2011. Aqueous biphasic systems involving alkylsulfate-based ionic liquids. J. Chem. Thermodyn. 43, 1565–1572.
Dimitrijević, A., Milićević, J., Jocić, A., Marić, S., Trtić-Petrović, T., Papović, S., Tot, A., Gadžurić, S., Vraneš, M., 2020. Further insight into the influence of functionalization and positional isomerism of pyridinium ionic liquids on the aqueous two-phase system equilibria. Fluid Phase Equilib. 512, 112520.
Dreyer, S., Kragl, U., 2008. Ionic liquids for aqueous two-phase extraction and stabilization of enzymes. Biotechnol. Bioeng. 99, 1416–1424.
Fang, M., Chen, Y., Pei, Y., Wang, Z., Zhuo, K., Bai, G., 2018. Construction of two-ionic liquid-based aqueous two-phase systems for extraction of pyritinol hydrochloride. J. Mol. Liq. 253, 228–232.
Faúndez, C.A., Fierro, E.N., Valderrama, J.O., 2016. Solubility of hydrogen sulfide in ionic liquids for gas removal processes using artificial neural networks. J. Environ. Chem. Eng. 4, 211–218.
Fister, S., Fuchs, S., Mester, P., Kilpeläinen, I., Wagner, M., Rossmanith, P., 2015. The use of ionic liquids for cracking viruses for isolation of nucleic acids. Sep. Purif. Technol. 155, 38–44.
Freire, M.G., 2016. Ionic-liquid-based aqueous biphasic systems. Springer.
Freire, M.G., Neves, C.M., Silva, A.M., Santos, L.M., Marrucho, I.M., Rebelo, L.P., Shah, J.K., Maginn, E.J., Coutinho, J.A., 2010. 1H NMR and molecular dynamics evidence for an unexpected interaction on the origin of salting-in/salting-out phenomena. J. Phys. Chem. B 114, 2004–2014.
Freire, M.G., Neves, C.M., Marrucho, I.M., Lopes, J.N.C., Rebelo, L.P.N., Coutinho, J.A., 2010. High-performance extraction of alkaloids using aqueous two-phase systems with ionic liquids. Green Chem. 12, 1715–1718.
Freire, M.G., Teles, A.R.R., Canongia Lopes, J.N., Rebelo, L.P.N., Marrucho, I.M., Coutinho, J.A., 2012. Partition coefficients of alkaloids in biphasic ionic-liquid-aqueous systems and their dependence on the Hofmeister series. Sep. Sci. Technol. 47, 284–291.
Freire, M.G., Claudio, A.F.M., Araujo, J.M., Coutinho, J.A., Marrucho, I.M., Lopes, J.N.C., Rebelo, L.P.N., 2012. Aqueous biphasic systems: a boost brought about by using ionic liquids. Chem. Soc. Rev. 41, 4966–4995.
Fu, J., Yang, Y.I., Zhang, J., Chen, Q., Shen, X., Gao, Y.Q., 2016. Structural Characteristics of homogeneous hydrophobic ionic liquid–HNO3–H2O ternary system: Experimental studies and molecular dynamics simulations. J. Phys. Chem. B 120, 5194–5202.
Gani, R., 2019. Group contribution-based property estimation methods: advances and perspectives. Curr. Opin. Chem. Eng. 23, 184–196.
Gao, J., Chen, L., Xin, Y., Yan, Z., 2014. Ionic liquid-based aqueous biphasic systems with controlled hydrophobicity: the polar solvent effect. J. Chem. Eng. Data 59, 2150–2158.
Gao, J., Chen, L., Yan, Z., 2015. Phase behavior of aqueous biphasic systems composed of ionic liquids and organic salts. J. Chem. Eng. Data 60, 464–470.
Gao, J., Guo, J., Nie, F., Ji, H., Liu, S., 2017. LCST-type phase behavior of aqueous biphasic systems composed of phosphonium-based ionic liquids and potassium phosphate. J. Chem. Eng. Data 62, 1335–1340.
Goja, A.M., Yang, H., Cui, M., Li, C., 2013. Aqueous two-phase extraction advances for bioseparation. J. Bioprocess. Biotechnol 4, 1–8.
Gómez, E., Domínguez, I., Domínguez, Á., Macedo, E.n.A., 2018. Ionic liquids-based aqueous biphasic systems with citrate biodegradable salts. J. Chem. Eng. Data 63, 1103-1108.
Gómez, E., Requejo, P.F., Tojo, E., Macedo, E.A., 2019. Recovery of flavonoids using novel biodegradable choline amino acids ionic liquids based ATPS. Fluid Phase Equilib. 493, 1–9.
Grilo, A.L., Raquel Aires-Barros, M., Azevedo, A.M., 2016. Partitioning in aqueous two-phase systems: fundamentals, applications and trends. Sep. Purif. Rev. 45, 68–80.
Guo, J., Xu, S., Qin, Y., Li, Y., Lin, X., He, C., Dai, S., 2020. The temperature influence on the phase behavior of ionic liquid based aqueous two-phase systems and its extraction efficiency of 2-chlorophenol. Fluid Phase Equilib. 506, 112394.
Gutowski, K.E., Broker, G.A., Willauer, H.D., Huddleston, J.G., Swatloski, R.P., Holbrey, J.D., Rogers, R.D., 2003. Controlling the aqueous miscibility of ionic liquids: aqueous biphasic systems of water-miscible ionic liquids and water-structuring salts for recycle, metathesis, and separations. J. Am. Chem. Soc. 125, 6632–6633.
Han, J., Yu, C., Wang, Y., Xie, X., Yan, Y., Yin, G., Guan, W., 2010b. Liquid–liquid equilibria of ionic liquid 1-butyl-3-methylimidazolium tetrafluoroborate and sodium citrate/tartrate/acetate aqueous two-phase systems at 298.15 K: experiment and correlation. Fluid Phase Equilib. 295, 98–103.
Han, J., Pan, R., Xie, X., Wang, Y., Yan, Y., Yin, G., Guan, W., 2010a. Liquid– liquid equilibria of ionic liquid 1-butyl-3-methylimidazolium tetrafluoroborate+ sodium and ammonium citrate aqueous two-phase systems at (298.15, 308.15, and 323.15) K. J. Chem. Eng. Data 55, 3749–3754.
Han, J., Wang, Y., Li, Y., Yu, C., Yan, Y., 2011. Equilibrium phase behavior of aqueous two-phase systems containing 1-alkyl-3-methylimidazolium tetrafluoroborate and ammonium tartrate at different temperatures: experimental determination and correlation. J. Chem. Eng. Data 56, 3679–3687.
Han, J., Wang, Y., Yu, C., Li, Y., Kang, W., Yan, Y., 2012. (Liquid+ liquid) equilibrium of (imidazolium ionic liquids+ organic salts) aqueous two-phase systems at T= 298.15 K and the influence of salts and ionic liquids on the phase separation. J. Chem. Thermodyn. 45, 59–67.
Han, J., Wang, Y., Chen, C., Kang, W., Liu, Y., Xu, K., Ni, L., 2014. (Liquid+ liquid) equilibria and extraction capacity of (imidazolium ionic liquids+ potassium tartrate) aqueous two-phase systems. J. Mol. Liq. 193, 23–28.
Iqbal, M., Tao, Y., Xie, S., Zhu, Y., Chen, D., Wang, X., Huang, L., Peng, D., Sattar, A., Shabbir, M.A.B., 2016. Aqueous two-phase system (ATPS): an overview and advances in its applications. Biological Procedures Online 18, 1–18.
Ito, Y., Kohno, Y., Nakamura, N., Ohno, H., 2013. Design of phosphonium-type zwitterion as an additive to improve saturated water content of phase-separated ionic liquid from aqueous phase toward reversible extraction of proteins. Int. J. Mol. Sci. 14, 18350–18361.
Jamehbozorg, B., Sadeghi, R., 2018. Evaluation of the effect of carbohydrates as renewable, none-charged and non-toxic soluting-out agents on the ionic-liquid-based ABS implementation. J. Mol. Liq. 255, 476–491.
João, K.G., Tomé, L.C., Gouveia, A.S., Marrucho, I.M., 2017. Aqueous biphasic systems of pyrrolidinium ionic liquids with organic acid-derived anions and K3PO4. J. Chem. Eng. Data 62, 1182–1188.
Lashkarbolooki, M., Vaferi, B., Rahimpour, M., 2011. Comparison the capability of artificial neural network (ANN) and EOS for prediction of solid solubilities in supercritical carbon dioxide. Fluid Phase Equilib. 308, 35–43.
Lei, Y., Zhou, Y., Wei, Z., Chen, Y., Guo, F., Yan, W., 2021. Optimal design of an ionic liquid (IL)-based aromatic extractive distillation process involving energy and economic evaluation. Ind. Eng. Chem. Res. 60, 3605–3616.
Li, Y., Gu, Y., Lu, X., 2015. Liquid–liquid equilibria for 1-butyl-4-methylpyridinium tetrafluoroborate and inorganic salts aqueous two-phase systems. J. Therm. Anal. Calorim. 122, 1455–1468.
Li, C., Han, J., Wang, Y., Yan, Y., Pan, J., Xu, X., Zhang, Z., 2010. Phase behavior for the aqueous two-phase systems containing the ionic liquid 1-butyl-3-methylimidazolium tetrafluoroborate and kosmotropic salts. J. Chem. Eng. Data 55, 1087–1092.
Li, Y., Huang, R., He, Z., Li, N., Lu, X., 2016. Phase behavior of an aqueous two-phase ionic liquid containing (N-butylpyridiniumtetrafluoroborate+ sulfate salts+ water) at different temperatures. J. Mol. Liq. 216, 174–184.
Li, S., Li, S., Zhai, Q., Jiang, Y., Hu, M., 2019. Solid–liquid and liquid–liquid equilibrium of the systems composed of [Cnmim] Cl/Br (n= 2, 4, 6, 8)+ Rb2SO4/Cs2SO4+ H2O. J. Mol. Liq. 273, 455–462.
Li, Y., Lu, X., Hao, J., Chen, C., 2013. Liquid-liquid equilibrium data for the ionic liquid N-ethyl-pyridinium bromide with several sodium salts and potassium salts. J. Chem. 2013.
Li, Y., Shu, X., Zhang, X., Guan, W., 2014. Liquid–liquid equilibria of the aqueous two-phase systems composed of the N-Ethylpyridinium tetrafluoroborate ionic liquid and ammonium sulfate/anhydrous sodium carbonate/sodium dihydrogen phosphate and water at 298.15 K. J. Chem. Eng. Data 59, 176–182.
Li, Y., Lu, X., Huang, R., Zhu, Q., Xie, Y., 2016. Phase behavior of inorganic salts sodium succinate and ammonium citrate in N-ethylpyridinium tetrafluoroborate solution at different temperatures. J. Chem. Eng. Data 61, 2380–2390.
Li, Y., Wu, Y., 2015. Experimental determination of phase equilibrium in aqueous two-phase systems containing ionic liquids and sodium salts at different temperatures. J. Chem. Eng. Data 60, 2003–2017.
Li, Y., Yang, L., Zhao, X., Guan, W., 2012. Liquid–liquid equilibria of ionic liquid N-ethylpyridinium tetrafluoroborate+ trisodium citrate/ammonium citrate tribasic/sodium succinate/sodium tartrate aqueous two-phase systems at 298.15 K. Thermochim. Acta 550, 5–12.
Li, Y., Zhang, M., Liu, Q., Su, H., 2013. Phase behaviour for aqueous two-phase systems containing the ionic liquid 1-butylpyridinium tetrafluoroborate/1-butyl-4-methylpyridinium tetrafluoroborate and organic salts (sodium tartrate/ammonium citrate/trisodium citrate) at different temperatures. J. Chem. Thermodyn. 66, 80–87.
Li, Y.-L., Zhang, M.-S., Su, H., Liu, Q., Guan, W.-S., 2013. Liquid–liquid equilibria of aqueous two-phase systems of the ionic liquid brominated N-ethyl pyridine and sodium dihydrogen phosphate, sodium sulfate, ammonium citrate, and

potassium tartrate at different temperatures: Experimental determination and correlation. Fluid Phase Equilib. 341, 70–77.
Li, Y., Zhang, M., Wu, J., Shi, J., Shen, C., 2014. Liquid–liquid equilibria of ionic liquid N-butylpyridinium tetrafluoroborate and disodium hydrogen phosphate/sodium chloride/sodium sulfate/ammonium sulfate aqueous two-phase systems at T= 298.15 K: Experiment and correlation. Fluid Phase Equilib. 378, 44–50.
Li, Y., Zhang, M., Su, H., Liu, Q., Shen, C., 2014. Liquid–liquid equilibria of ionic liquid 1-butyl-pyridinium tetrafluoroborate and ammonium citrate/trisodium citrate/sodium succinate/sodium acetate aqueous two-phase systems at 303.15 K: Experiment and correlation. J. Mol. Liq. 199, 115–122.
Li, Y., Xu, Z., Luo, Q., Lu, X., Hu, J., 2016. Phase diagram of ionic liquid aqueous two-phase systems with N-butylpyridinium tetrafluoroborate, ammonium Citrate/Sodium acetate, and water from 308.15 K to 328.15 K. Thermochim. Acta 632, 72–78.
Li, Y., Lu, X., Wu, J., 2016. Effect of Temperature on the Liquid-Liquid Equilibrium of the Ternary Aqueous System Containing N-Butylpyridinium Tetrafluoroborate and Sodium Dihydrogen Phosphate. Int. J. Thermophys. 37, 16.
Li, Y., Lu, X., He, W., Huang, R., Zhao, Y., Wang, Z., 2016. Influence of the salting-out ability and temperature on the liquid-liquid equilibria of aqueous two-phase systems based on ionic liquid-organic salts–water. J. Chem. Eng. Data 61, 475–486.
Li, Y., Huang, R., Zhu, Q., Yu, Y., Hu, J., 2017. Phase behavior at different temperatures of an aqueous two-phase ionic liquid containing ([BPy] NO3+ ammonium sulfate and sodium sulfate+ water). J. Chem. Eng. Data 62, 796–803.
Liang, R., Bao, Z., Su, B., Xing, H., Yang, Q., Yang, Y., Ren, Q., 2013. Feasibility of ionic liquids as extractants for selective separation of vitamin D3 and tachysterol3 by solvent extraction. J. Agric. Food. Chem. 61, 3479–3487.
Lin, X., Wang, Y., Zeng, Q., Ding, X., Chen, J., 2013. Extraction and separation of proteins by ionic liquid aqueous two-phase system. Analyst 138, 6445–6453.
Liu, X., Chen, Y., Zeng, S., Zhang, X., Zhang, S., Liang, X., Gani, R., Kontogeorgis, G.M., 2020. Structure optimization of tailored ionic liquids and process simulation for shale gas separation. AlChE J. 66, e16794.
Liu, X., Chen, Y., Zeng, S., Zhang, X., Liang, X., Gani, R., Kontogeorgis, G.M., 2021. Separation of NH3/CO2 from melamine tail gas with ionic liquid: Process evaluation and thermodynamic properties modelling. Sep. Purif. Technol. 119007.
Liu, B., Jin, N., 2016. The applications of ionic liquid as functional material: a review. Curr. Org. Chem. 20, 2109–2116.
Liu, Q., Ni, L., Han, J., Wang, Y., Tang, X., Zhang, W., Xie, X., 2016. Phase behavior of aqueous two-phase systems composed by 1-allyl-3-methylimidazolium chloride and aqueous potassium salts at various temperatures. J. Chem. Eng. Data 61, 3698–3703.
Louros, C.L., Cláudio, A.F.M., Neves, C.M., Freire, M.G., Marrucho, I.M., Pauly, J., Coutinho, J.A., 2010. Extraction of biomolecules using phosphonium-based ionic liquids+ K3PO4 aqueous biphasic systems. Int. J. Mol. Sci. 11, 1777–1791.
Lv, H., Jiang, Z., Li, Y., Ren, B., 2012. Liquid–liquid equilibria of the aqueous two-phase systems of ionic liquid 1-butyl-3-methylimidazolium tetrafluoroborate and sodium dihydrogen phosphate/disodium hydrogen phosphate or their mixtures. J. Chem. Eng. Data 57, 2379–2386.
Lv, H., Guo, D., Jiang, Z., Li, Y., Ren, B., 2013. Phase behavior of aqueous two-phase systems composed of 1-ethyl-3-methylimidazolium tetrafluoroborate and phosphate-based salts at different temperatures. Fluid Phase Equilib. 341, 23–29.
Magalhães, F.F., Tavares, A.P., Freire, M.G., 2020. Advances in aqueous biphasic systems for biotechnology applications. Curr. Opin. Green Sustain. Chem. 100417.
Malekghasemi, S., Mokhtarani, B., Hamzehzadeh, S., Hajfarajollah, H., Sharifi, A., Mirzaei, M., 2016. Phase diagrams of aqueous biphasic systems composed of ionic liquids and dipotassium carbonate at different temperatures. Fluid Phase Equilib. 415, 193–202.
Malekghasemi, S., Mokhtarani, B., Hamzehzadeh, S., Sharifi, A., Mirzaei, M., 2016. Liquid–liquid equilibria of aqueous biphasic systems of ionic liquids and dipotassium hydrogen phosphate at different temperatures: Experimental study and thermodynamic modeling. J. Mol. Liq. 219, 95–103.
Meng, X., Ju, Z., Zhang, S., Liang, X., von Solms, N., Zhang, X., Zhang, X., 2019. Efficient transformation of CO 2 to cyclic carbonates using bifunctional protic ionic liquids under mild conditions. Green Chem. 21, 3456–3463.
Merchuk, J.C., Andrews, B.A., Asenjo, J.A., 1998. Aqueous two-phase systems for protein separation: studies on phase inversion. J. Chromatogr. B Biomed. Sci. Appl. 711, 285–293.
Mourão, T., Cláudio, A.F.M., Boal-Palheiros, I., Freire, M.G., Coutinho, J.A., 2012. Evaluation of the impact of phosphate salts on the formation of ionic-liquid-based aqueous biphasic systems. J. Chem. Thermodyn. 54, 398–405.
Mulero, Á., Cachadiña, I., Valderrama, J.O., 2017. Artificial neural network for the correlation and prediction of surface tension of refrigerants. Fluid Phase Equilib. 451, 60–67.
Nadar, S.S., Pawar, R.G., Rathod, V.K., 2017. Recent advances in enzyme extraction strategies: a comprehensive review. Int. J. Biol. Macromol. 101, 931–957.
Noshadi, S., Sadeghi, R., 2017. Evaluation of the capability of ionic liquid–amino acid aqueous systems for the formation of aqueous biphasic systems and their applications in extraction. J. Phys. Chem. B 121, 2650–2664.
Okuniewski, M., Paduszynski, K., Domanska, U., 2016. Effect of cation structure in trifluoromethanesulfonate-based ionic liquids: density, viscosity, and aqueous biphasic systems involving carbohydrates as "salting-out" agents. J. Chem. Eng. Data 61, 1296–1304.
Patinha, D., Alves, F., Rebelo, L., Marrucho, I., 2013. Ionic liquids based aqueous biphasic systems: Effect of the alkyl chains in the cation versus in the anion. J. Chem. Thermodyn. 65, 106–112.
Pei, Y., Wang, J., Liu, L., Wu, K., Zhao, Y., 2007. Liquid− liquid equilibria of aqueous biphasic systems containing selected imidazolium ionic liquids and salts. J. Chem. Eng. Data 52, 2026–2031.
Pei, Y., Wang, J., Wu, K., Xuan, X., Lu, X., 2009. Ionic liquid-based aqueous two-phase extraction of selected proteins. Sep. Purif. Technol. 64, 288–295.
Pei, Y., Li, Z., Liu, L., Wang, J., 2012. Partitioning behavior of amino acids in aqueous two-phase systems formed by imidazolium ionic liquid and dipotassium hydrogen phosphate. J. Chromatogr. A 1231, 2–7.
Peng, D., Picchioni, F., 2020. Prediction of toxicity of Ionic Liquids based on GC-COSMO method. J. Hazard. Mater. 398, 122964.
Plechkova, N.V., Seddon, K.R., 2007. Ionic liquids:"designer" solvents for green chemistry. Methods and Reagents for Green Chemistry, 105–130.
Quental, M.V., Caban, M., Pereira, M.M., Stepnowski, P., Coutinho, J.A., Freire, M.G., 2015. Enhanced extraction of proteins using cholinium-based ionic liquids as phase-forming components of aqueous biphasic systems. Biotechnol. J. 10, 1457–1466.
Quental, M.V., Passos, H., Kurnia, K.A., Coutinho, J.o.A., Freire, M.G., 2015. Aqueous biphasic systems composed of ionic liquids and acetate-based salts: phase diagrams, densities, and viscosities. J. Chem. Eng. Data 60, 1674-1682.
Raja, S., Murty, V.R., Thivaharan, V., Rajasekar, V., Ramesh, V., 2011. Aqueous two phase systems for the recovery of biomolecules–a review. Sci. Technol. 1, 7–16.
Ren, G., Gong, X., Wang, B., Chen, Y., Huang, J., 2015. Affinity ionic liquids for the rapid liquid–liquid extraction purification of hexahistidine tagged proteins. Sep. Purif. Technol. 146, 114–120.
Rogers, R.D., Seddon, K.R., 2003. Ionic liquids–solvents of the future?. Science 302, 792–793.
Sadeghi, R., Golabiazar, R., Shekaari, H., 2010. The salting-out effect and phase separation in aqueous solutions of tri-sodium citrate and 1-butyl-3-methylimidazolium bromide. J. Chem. Thermodyn. 42, 441–453.
Sedghamiz, M.A., Rasoolzadeh, A., Rahimpour, M.R., 2015. The ability of artificial neural network in prediction of the acid gases solubility in different ionic liquids. J. CO2 Util. 9, 39–47.
Shill, K., Padmanabhan, S., Xin, Q., Prausnitz, J.M., Clark, D.S., Blanch, H.W., 2011. Ionic liquid pretreatment of cellulosic biomass: enzymatic hydrolysis and ionic liquid recycle. Biotechnol. Bioeng. 108, 511–520.
Sintra, T.E., Cruz, R., Ventura, S.P., Coutinho, J.A., 2014. Phase diagrams of ionic liquids-based aqueous biphasic systems as a platform for extraction processes. J. Chem. Thermodyn. 77, 206–213.
Song, Z., Zhang, C., Qi, Z., Zhou, T., Sundmacher, K., 2018. Computer-aided design of ionic liquids as solvents for extractive desulfurization. AlChE J.
Song, Z., Li, X., Chao, H., Mo, F., Zhou, T., Cheng, H., Chen, L., Qi, Z., 2019. Computer-aided ionic liquid design for alkane/cycloalkane extractive distillation process. Green Energy Environ. 4, 154–165.
Song, Z., Shi, H., Zhang, X., Zhou, T., 2020. Prediction of CO2 solubility in ionic liquids using machine learning methods. Chem. Eng. Sci. 223, 115752.
Tang, X., Han, J., Hu, Y., Wang, Y., Lu, Y., Chen, T., Ni, L., 2014. The study of phase behavior of aqueous two-phase system containing [Cnmim] BF4 (n= 2, 3, 4) +(NH4) 2SO4+ H2O at different temperatures. Fluid Phase Equilib. 383, 100–107.
Tatar, A., Naseri, S., Bahadori, M., Hezave, A.Z., Kashiwao, T., Bahadori, A., Darvish, H., 2016. Prediction of carbon dioxide solubility in ionic liquids using MLP and radial basis function (RBF) neural networks. J. Taiwan Inst. Chem. Eng. 60, 151–164.
Tomé, L.I., Varanda, F.R., Freire, M.G., Marrucho, I.M., Coutinho, J.A., 2009. Towards an understanding of the mutual solubilities of water and hydrophobic ionic liquids in the presence of salts: the anion effect. J. Phys. Chem. B 113, 2815–2825.
Vargas, S.J., Quintao, J.C., Ferreira, G.M., Da Silva, L.H., Hespanhol, M.C., 2019. Lanthanum and cerium separation using an aqueous two-phase system with ionic liquid. J. Chem. Eng. Data 64, 4239–4246.
Vekariya, R.L., 2017. A review of ionic liquids: Applications towards catalytic organic transformations. J. Mol. Liq. 227, 44–60.
Ventura, S.P., e Silva, F.A., Quental, M.V., Mondal, D., Freire, M.G., Coutinho, J.A., 2017. Ionic-liquid-mediated extraction and separation processes for bioactive compounds: past, present, and future trends. Chem. Rev. 117, 6984-7052.
Ventura, S.P., Neves, C.M., Freire, M.G., Marrucho, I.M., Oliveira, J., Coutinho, J.A., 2009. Evaluation of anion influence on the formation and extraction capacity of ionic-liquid-based aqueous biphasic systems. J. Phys. Chem. B 113, 9304–9310.
Ventura, S.P., Sousa, S.G., Serafim, L.S., Lima, Á.S., Freire, M.G., Coutinho, J.A., 2011. Ionic liquid based aqueous biphasic systems with controlled pH: the ionic liquid cation effect. J. Chem. Eng. Data 56, 4253–4260.
Wang, Y., Xu, X., Yan, Y., Han, J., Zhang, Z., 2010. Phase behavior for the [Bmim] BF4 aqueous two-phase systems containing ammonium sulfate/sodium carbonate salts at different temperatures: Experimental and correlation. Thermochim. Acta 501, 112–118.
Wang, Y., Han, J., Liu, J., Hu, Y., Sheng, C., Wu, Y., 2013. Liquid–liquid equilibrium phase behavior of iminazolium-based ionic liquid aqueous two-phase systems composed of 1-alkyl-3-methyl imidazolium tetrafluoroborate and different electrolytes ZnSO4, MgSO4 and Li2SO4 at 298.15 K: Experimental and correlation. Thermochim. Acta 557, 68–76.
Wang, J., Pei, Y., Zhao, Y., Hu, Z., 2005. Recovery of amino acids by imidazolium based ionic liquids from aqueous media. Green Chem. 7, 196–202.

Wang, Z., Song, Z., Zhou, T., 2021. Machine learning for ionic liquid toxicity prediction. Processes 9, 65.
Wang, T., Zhang, D., Cai, Y., Han, J., Liu, Q., Wang, Y., 2016. Thermodynamic equilibrium of aqueous two-phase systems composed of [C4mim] BF4+ MgCl2/Na2WO4+ H2O at different temperatures. J. Chem. Eng. Data 61, 1821–1828.
Wang, L., Zhu, H., Ma, C., Yan, Y., Wang, Q., 2012. Measurement and correlation of phase diagram data for aqueous two-phase systems containing 1-ethyl-3-methylimidazolium dimethyl phosphate+ K3PO4/K2HPO4/K2CO3+ H2O ionic liquids at (298.15, 308.15, and 318.15) K. J. Chem. Eng. Data 57, 681–687.
Wu, X., Liu, Y., Zhao, Y., Cheong, K.-L., 2018. Effect of salt type and alkyl chain length on the binodal curve of an aqueous two-phase system composed of imidazolium ionic liquids. J. Chem. Eng. Data 63, 3297–3304.
Wu, B., Zhang, Y.M., Wang, H.P., 2008. Aqueous biphasic systems of hydrophilic ionic liquids+ sucrose for separation. J. Chem. Eng. Data 53, 983–985.
Wu, D., Zhou, Y., Cai, P., Shen, S., Pan, Y., 2015. Specific cooperative effect for the enantiomeric separation of amino acids using aqueous two-phase systems with task-specific ionic liquids. J. Chromatogr. A 1395, 65–72.
Xu, W., Cao, H., Ren, G., Xie, H., Huang, J., Li, S., 2014. An AIL/IL-based liquid/liquid extraction system for the purification of His-tagged proteins. Appl. Microbiol. Biotechnol. 98, 5665–5675.
Xu, S., Zhu, Q., Luo, Q., Li, Y., 2019. Influence of ions and temperature on aqueous biphasic systems containing ionic liquid and ammonium sulfate. J. Chem. Eng. Data 64, 3139–3147.
Yan, J.-K., Ma, H.-L., Pei, J.-J., Wang, Z.-B., Wu, J.-Y., 2014. Facile and effective separation of polysaccharides and proteins from Cordyceps sinensis mycelia by ionic liquid aqueous two-phase system. Sep. Purif. Technol. 135, 278–284.
Yang, Q., Xing, H., Cao, Y., Su, B., Yang, Y., Ren, Q., 2009. Selective separation of tocopherol homologues by liquid− liquid extraction using ionic liquids. Ind. Eng. Chem. Res. 48, 6417–6422.
Yang, Q., Xing, H., Su, B., Yu, K., Bao, Z., Yang, Y., Ren, Q., 2012. Improved separation efficiency using ionic liquid–cosolvent mixtures as the extractant in liquid–liquid extraction: A multiple adjustment and synergistic effect. Chem. Eng. J. 181, 334–342.
Yang, Q., Xing, H., Su, B., Bao, Z., Wang, J., Yang, Y., Ren, Q., 2013. The essential role of hydrogen-bonding interaction in the extractive separation of phenolic compounds by ionic liquid. AIChE J. 59, 1657–1667.
Yao, T., Huang, X., Zang, H., Song, H., Yao, S., 2017. Measurement and correlation of phase equilibria in aqueous two-phase systems containing functionalized magnetic ionic liquids and K2HPO4/K2CO3/Na2CO3 at 298.15 K. J. Mol. Liq. 231, 411–418.
Yu, C., Han, J., Hu, S., Yan, Y., Li, Y., 2011. Phase diagrams for aqueous two-phase systems containing the 1-ethyl-3-methylimidazolium tetrafluoroborate/1-propyl-3-methylimidazolium tetrafluoroborate and trisodium phosphate/sodium sulfite/sodium dihydrogen phosphate at 298.15 K: experiment and correlation. J. Chem. Eng. Data 56, 3577–3584.
Zafarani-Moattar, M.T., Hamzehzadeh, S., 2007. Liquid− liquid equilibria of aqueous two-phase systems containing 1-butyl-3-methylimidazolium bromide and potassium phosphate or dipotassium hydrogen phosphate at 298.15 K. J. Chem. Eng. Data 52, 1686–1692.
Zafarani-Moattar, M.T., Hamzehzadeh, S., 2009. Phase diagrams for the aqueous two-phase ternary system containing the ionic liquid 1-butyl-3-methylimidazolium bromide and tri-potassium citrate at T=(278.15, 298.15, and 318.15) K. J. Chem. Eng. Data 54, 833–841.
Zafarani-Moattar, M.T., Hamzehzadeh, S., 2010. Salting-out effect, preferential exclusion, and phase separation in aqueous solutions of chaotropic water-miscible ionic liquids and kosmotropic salts: Effects of temperature, anions, and cations. J. Chem. Eng. Data 55, 1598–1610.
Zafarani-Moattar, M.T., Hamzehzadeh, S., 2011. Partitioning of amino acids in the aqueous biphasic system containing the water-miscible ionic liquid 1-butyl-3-methylimidazolium bromide and the water-structuring salt potassium citrate. Biotechnol. Progr. 27, 986–997.
Zafarani-Moattar, M.T., Sarmad, S., 2011. Osmotic and activity coefficient of 1-ethyl-3-methylimidazolium chloride in aqueous solutions of tri-potassium phosphate, potassium carbonate, and potassium chloride at T= 298.15 K. Calphad 35, 331–341.
Zhang, J., Zhang, Y., Chen, Y., Zhang, S., 2007. Mutual coexistence curve measurement of aqueous biphasic systems composed of [bmim][BF4] and glycine, L-serine, and L-proline, respectively. J. Chem. Eng. Data 52, 2488–2490.
Zhang, Y., Zhang, S., Chen, Y., Zhang, J., 2007. Aqueous biphasic systems composed of ionic liquid and fructose. Fluid Phase Equilib. 257, 173–176.
Zhao, Y., Zhao, J., Huang, Y., Zhou, Q., Zhang, X., Zhang, S., 2014. Toxicity of ionic liquids: database and prediction via quantitative structure–activity relationship method. J. Hazard. Mater. 278, 320–329.
Zhao, Y., Gao, J., Huang, Y., Afzal, R.M., Zhang, X., Zhang, S., 2016. Predicting H 2 S solubility in ionic liquids by the quantitative structure–property relationship method using S σ-profile molecular descriptors. RSC Adv. 6, 70405–70413.